Technical University of Munich

TUM - School of Engineering and Design

Chair of Computational Modeling and Simulation

Parameter-Based Model Reconstruction from Space-wise Segmented Point Cloud

Master thesis

for the Master of Science Course Civil Engineering

Autor:	Ahmed Ibrahim
Matriculation number:	03754821
Supervisor	M. Sc Jiabin Wu
	M. Sc. Mansour Mehranfar
	Paulina Sala (ZM-I)
Examiners:	Prof. Dr.-Ing. André Borrmann
Date of issue:	15. April 2023
Submission date:	05. November 2023

Abstract

Assessing indoor spaces in existing buildings has recently evolved beyond conventional measurement techniques. Contemporary practices now involve point cloud utilizing laser scanners, enabling precise spatial data capture. This thesis delves into transforming segmented point cloud data into parametric 3D models. This transformation is accomplished via a structured framework. The primary objective of this research is to harness the potential of segmented point cloud data for parametric modeling of indoor space. This modeling process plays a crucial role when the functionality of a building undergoes changes or when there is a need to enhance facility management workflows and achieve additional objectives. The input of the proposed framework includes 3D semantic segmented and space-wise labeled point clouds and the adjacency matrices among corresponding spaces. The outcome of the study consists of parametric models, which provide a detailed representation of the indoor environment, such as space dimensions, height, boundary thickness, and lengths. The proposed method is tested and validated on different datasets. The results show the effectiveness of the proposed method in creating a parametric model. The average accuracy of the constructed walls in the constructed model and the reference model is 0.13 m in length and less than 0.1 m in width, and height.

Zusammenfassung

Die Bewertung von Innenräumen in bestehenden Gebäuden hat sich in jüngster Zeit über herkömmliche Messverfahren hinaus entwickelt. Heute werden Punktwolken mit Hilfe von Laserscannern erstellt, die eine präzise Erfassung räumlicher Daten ermöglichen. Diese Arbeit befasst sich mit der Umwandlung von segmentierten Punktwolkendaten in parametrische 3D-Modelle. Diese Umwandlung wird mit Hilfe eines strukturierten Rahmens durchgeführt. Das primäre Ziel dieser Arbeit ist es, das Potenzial von segmentierten Punktwolkendaten für die parametrische Modellierung von Innenräumen zu nutzen. Dieser Modellierungsprozess spielt eine entscheidende Rolle, wenn sich die Funktionalität eines Gebäudes ändert oder wenn die Arbeitsabläufe im Facility Management verbessert und zusätzliche Ziele erreicht werden sollen. Die Eingabe des vorgeschlagenen Rahmens umfasst semantisch segmentierte und raumweise beschriftete 3D-Punktwolken und die Adjazenz Matrizen zwischen den entsprechenden Räumen. Das Ergebnis der Studie besteht aus parametrischen Modellen, die eine detaillierte Darstellung der Innenraumumgebung liefern, z. B. Raumabmessungen, Höhe, Grenzdicke und -länge. Die vorgeschlagene Methode wurde an verschiedenen Datensätzen getestet und validiert. Die Ergebnisse zeigen die Wirksamkeit der vorgeschlagenen Methode bei der Erstellung eines parametrischen Modells. Die durchschnittliche Genauigkeit der konstruierten Wände im konstruierten Modell und im Referenzmodell beträgt 0,13 m in der Länge und weniger als 0,1 m in der Breite und in der Höhe.

Contents

1 Introduction 13
1.1 Preface 13
1.2 Motivation 14
1.3 Research objectives....................15
1.4 Thesis structure 15

2 State of the art 16
2.1 Building Information Modeling....................16
2.1.1 Evolution of BIM....................17
2.1.2 BIM Dimensions and LODs....................18
2.1.3 BIM and facility management....................19
2.2 Digital Twin 20
2.2.1 Digital Twin definition....................20
2.2.2 Integration of DT with different technologies....................21
2.2.3 DT life cycle 23
2.3 Scan-to-BIM....................24
2.3.1 Point cloud....................24
2.3.2 Point cloud acquisition 26
2.3.3 Point cloud preprocessing....................29
2.3.4 Point cloud processing....................32
2.3.5 Model reconstruction....................35

3 Methodology 39
3.1 Data preparation....................40
3.1.1 Data acquisition 40
3.1.2 Point cloud preprocessing....................40
3.1.3 Point cloud segmentation....................41
3.1.4 Rooms initial characteristics 43
3.2 Spaces placement 44
3.2.1 Placement of the primary room....................44

3.2.2 Iterative placement of the adjacent spaces 45
3.2.3 Check the reliability of spaces 47
3.2.4 Adjust spaces' boundaries 48
3.3 Boundaries parameters 49
3.3.1 Common edge reduction 49
3.3.2 Refinning the boundaries of spaces 50
3.3.3 Wall Parameters 51
3.4 Tools 53

4 Results 54
4.1 Inputs 54
4.2 Data set 1 56
4.3 Data set 2 58
4.4 Data set 3 61
4.5 Data set 4 64
4.6 Quantitative evaluation of model reconstruction 66

5 Conclusion and future work 67
5.1 Conclusion 67
5.2 Limitations and future works 69

References 71

Appendix A 83
A .1 Overlapping wall algorithm 83
A .2 Reliability check algorithm 84
A .3 Get internal wall algorithm 86

Appendix B 87
B .1 Convex hull algorithm 87

List of Figures

Figure 2. 1: Example of the BIM model 17

Figure 2. 2: BIM dimensions 18

Figure 2. 3: BIM Levels of development as related to all phases of the building lifecycle 19

Figure 2. 4: The relationship between DT and BIM 21

Figure 2. 5: Life cycle of physical and digital building twins 23

Figure 2. 6: Sample indoor point cloud data. 25

Figure 2. 7: Point cloud of the existing building environment (overlapping with the BIM model) 26

Figure 2. 8: Image-derived point cloud sample 27

Figure 2. 9: Dense TLS indoor point cloud of a building at Oregon State University 28

Figure 2. 10: Point cloud captured by RGB-D camera in typical indoor scenes 29

Figure 2. 11: Results of outliers' removal on a horse model 30

Figure 2. 12: Point cloud subsampling 31

Figure 2. 13 Point cloud segmentation 32

Figure 2. 14: Segmentation of 3D point cloud using geometric primitive fitting 34

Figure 2. 15: Semantic segmentation of indoor point cloud. 34

Figure 2. 16: 3D point cloud of a facility 36

Figure 2. 17: Detecting the parameters of the shared wall between rooms 38

Figure 3. 1: The workflow of the framework 39

Figure 3. 2: Raw point cloud of Data set 1 40

Figure 3. 3: 3D view of ceiling and wall semantic point cloud 41

Figure 3. 4: Top view of the space-wise point cloud 42

Figure 3. 5: Data set 1 – Rooms Characteristics 45

Figure 3. 6: Procedure of space alignment – first series of iteration 46

Figure 3. 7: Procedure of space alignment – second series of iteration 46

Figure 3. 8: Adjacent spaces around the primary room 47

Figure 3. 9: Check the reliability of space placement 48

Figure 3. 10: Adjustment of spaces' boundaries 49

Figure 3. 11: Merging the common walls 50

Figure 3. 12: Refinning the boundaries of spaces 51

Figure 3. 13: Top view of reconstructed BIM model 53

Figure 4. 1: Raw point cloud of data set 1 54

Figure 4. 2: Raw point cloud of data set 2 54

Figure 4. 3: Raw point cloud of data set 3 54

Figure 4. 4: Raw point cloud of data set 4 54

Figure 4. 5: The semantic segmented point cloud of Data set 1 56

Figure 4. 6: The reconstructed BIM model of data set 1 57

Figure 4. 7: Top view of rooms and walls of Data set 1 57

Figure 4. 8: The semantic segmented point cloud of Data set 2 58

Figure 4. 9: The reconstructed BIM model of data set 2 59

Figure 4. 10: A top view of rooms and walls of Data set 2 60

Figure 4. 11: The semantic segmented point cloud of Data set 3 61

Figure 4. 12: The reconstructed BIM model of data set 3. 62

Figure 4. 13: Top view of labeled rooms and walls of Data set 3 63

Figure 4. 14: The semantic segmented point cloud of Data set 4 64

Figure 4. 15: The reconstructed BIM model of data set 4. 65

Figure 4. 16: Top view of labeled rooms and walls of Data set 4 65

Figure 5. 1: Run time analysis of the 4 Data sets 67

Figure 5. 2: Walls Parameter differences between the reconstructed and the reference BIM models 68

Figure 5. 3: Difference in wall heights of the same room 69

Figure 5. 4: Alternative procedure for points assignment to the corresponding walls 70

List of Tables

Table 3. 1: An example of points extracted from semantic point cloud - Data set 1 . 42

Table 3. 2: Three points extracted from space-wise floor point cloud....................... 43

Table 3. 3: Adjacency matrix - Data set 1... 43

Table 3. 4: Data set 1 – Rooms Characteristics 44

Table 4. 1: Data sets input data... 55

Table 4. 2: Quantitative evaluation of model construction 66

List of Abbreviations

BIM	Building Information Modelling
DT	Digital Twin
FM	Facility Management
IFMA	International Facility Management Association
IoT	Internet of Things
VR	Virtual Reality
AR	Augmented Reality
NIST	National Institute of Standards and Technology - (United States of America)
AEC	Architecture, Engineering, and Construction
DTP	Digital Twin Prototype
DTI	Digital Twin Instance
LOD	Level of Development
LOG	Level of Geometry
LOI	List of Information
API	Application Programming Interface
CAD	Computer-Aided Design
WSN	Wireless Sensor Networks
RANSAC	Random Sample Consensus

ICP	Iterative Closest Point
CSG	Constructive Solid Geometry
SVM	Support Vector Machine
DSMs	Digital Surface Models
DEMs	Digital Elevation Models
LiDAR	Light Detection and Ranging
GNSS	Global Navigation Satellite System
IMU	International Measurement Units
SLAM	Simultaneous Localization and Mapping
PCSS	Point Cloud Semantic Segmentation
CNNs	Convolutional Neural Networks
HD map	high-definition map

1 Introduction

1.1 Preface

BIM and DT are pivotal technologies designed to offer virtual digital representations of constructed structures and buildings for vital functions such as examination, strategizing, administration, and regulation (Bortoluzzi et al., 2019) (Boje et al., 2020). These technologies have garnered substantial attention due to their transformative potential in building design, construction, and facility management, offering enhanced insights and capabilities (Sepasgozar et al., 2023). BIM provides a collaborative way for multidisciplinary information storing, sharing, exchanging, and managing throughout the real estate asset life cycle (L. Tang et al., 2017).

DT is a virtual depiction of a tangible entity, mechanism, or operation, offering immediate observations and examination in real-time (Voas et al., 2021). It is a powerful tool across various industries, including manufacturing and construction. Digital twins enable continuous monitoring, analysis, and optimization of physical assets and operations. By integrating data from sensors and other sources, they facilitate data-driven decision-making and predictive maintenance (van Dinter et al., 2022). Digital twins are becoming increasingly essential in complex systems, offering opportunities for improved building efficiency, sustainability, and innovation (Michael Grieves and John Vickers, 2017). The process of building digital twinning via laser scanner point cloud datasets involves the creation of a virtual duplicate of a building's physical assets. This is accomplished by utilizing data acquired from both indoor and exterior spaces. Despite the potential advantages offered by high-density point cloud collection in terms of speed and precision, it is worth noting that scanning large-scale buildings remains a challenging endeavor. This is primarily due to factoring space layouts, clutter, and obstructions (Ochmann et al., 2016).

In recent years, advanced technologies like BIM and DT have been used to improve the life cycle of the building (Barazzetti, 2016). One popular method for creating BIM models from an existing environment is known as "SCAN-to-BIM," which involves using remote sensing technologies such as laser scanning and photogrammetry to capture 3D data from a physical building and then processing that data to create a BIM model with coherent geometry (Pepe et al., 2021).

In this thesis, we expound upon the procedural intricacies of converting segmented point cloud data into parametric models. This process serves as the cornerstone for the comprehensive reconstruction of indoor spaces. Our primary objective revolves around architectural structures, evolving functional requirements, and streamlining facility management workflows. The methodology is designed to fortify building management practices, enhance operational efficiency, and promote sustainability within the dynamic milieu of AEC environments.

1.2 Motivation

The construction sector grapples with harmonizing the digital and physical realms. A significant hurdle lies in the disconnect between data analysis and subsequent actions, leading to fragmented information, redundant data, and inefficiencies spanning the entire building lifecycle (J. Zhang et al., 2022).

Creating a building floor plan is considered an essential initial step in constructing a 3D virtual DT model, as it provides the basic layout and structure of the building (Mehranfar et al., 2022). Once the floor plan is established, additional parameters such as wall thickness, ceiling height, and material properties can be added to a parametric model to create a more comprehensive representation of the building. This digital parametric model has numerous applications in the AEC industry (Adán et al., 2023).

The generated digital parametrized model can be used for virtual reality applications, such as developing a hybrid model for building energy consumption prediction considering building envelope retrofitting, indoor navigation, robotic applications, and remote collaboration (Donato, 2015).

The process of parametric modeling using space-wise segmented point cloud data represents a pivotal methodology in generating precise and intricate 3D representations of building indoor environments. The parametric model encompasses variables for walls’ locations, dimensions, and areas of space. These parametric models empower users to customize the model to suit diverse objectives, hold substantial utility across various applications.

1.3 Research objectives

The objective of this thesis is to create a parametric model of the building indoor environment based on segmented point cloud data. This endeavor encompasses several vital steps, including the use of the segmented point cloud of the indoor environment to extract the adjacency matrix for the relation of the spaces and the extraction of geometric attributes such as width, length, height, and the quantification of walls. The proposed methodology initially entails the establishment of spatial boundaries. Subsequently, the model is fine-tuned to align with the data points by manipulating global wall parameters for further layout optimization.

These data play a pivotal role in the construction of a comprehensive 3D digital representation of the built environment. The approach adopted in this study effectively addresses various challenges encountered in previous solutions, including issues related to data volume.

1.4 Thesis structure

The present thesis is structured as follows:

- Chapter 2 provides an initial theoretical foundation for BIM and DT technologies, exploring the complexity of point cloud technology with a focus on the segmentation process. Additionally, it reviews relevant research on the creation of parameterized models from indoor point clouds.

- Chapter 3 focuses on the proposed methodology, intricately workflow underpinning the proposed approach and outlines the practical application of the proposed methodology, detailing the steps taken to execute the research plan.

- Chapter 4 presents the empirical findings, data analysis, and their significance in addressing the research objectives and supporting or refuting the methodology.

- Chapter 5 addresses the entirety of the research inquiries, engages in a comprehensive discussion of the research findings, and encapsulates the contributions made by this thesis. Additionally, it delineates the constraints inherent in the proposed methodology and contemplates prospects for its ongoing enhancement.

2 State of the art

This chapter delves into the theoretical foundation and concepts to foster a more profound comprehension of this thesis's terminologies, techniques, and procedures.

2.1 Building Information Modeling

BIM represents a comprehensive digital depiction of a constructed facility, rich in informational content. It typically encompasses the 3D geometry of building elements at a specified level of detail. Additionally, it includes non-physical entities like spaces and zones, a hierarchical project structure, and schedules. Objects within this model are generally associated with precise semantic parameters, such as component types, materials, technical attributes, costs, and the relationships between components and other physical entities. Consequently, the term BIM encompasses both the process of creating these parametric digital building models and the processes involved in maintaining, utilizing, and exchanging them throughout the entire lifespan of the constructed facility (Borrmann et al., 2018).

The parametric BIM model is crucial for representing and managing building information. BIM Parameters allow for the definition and control of various aspects of building elements, from their geometric characteristics to their associated data. The ability to define and manipulate these parameters is central to the efficiency and accuracy of the BIM process (Mora et al., 2020). Parametric BIM enhances design efficiency through intelligent modeling. The ability to create designs driven by parameters and rules ensures consistency and reduces design errors (Eastman et al., 2008). These models enable rapid prototyping, iteration, and automation of design processes, ultimately saving time and resources (Becerik-Gerber et al., 2012). It fosters improved collaboration among AEC stakeholders. The models are accessible to all project team members, allowing architects, engineers, and contractors to work in a shared environment. Collaborative decision-making based on real-time data leads to a reduction in conflicts and rework (Azhar, 2011). Parametric BIM provides precise cost estimation capabilities by integrating cost data with the model (Eastman et al., 2008). This integration allows for real-time cost tracking and helps project managers make informed decisions on budget allocation (Elmualim et al., 2010). Figure 2.1 shows a BIM model of two floors and a basement containing walls and floor objects.

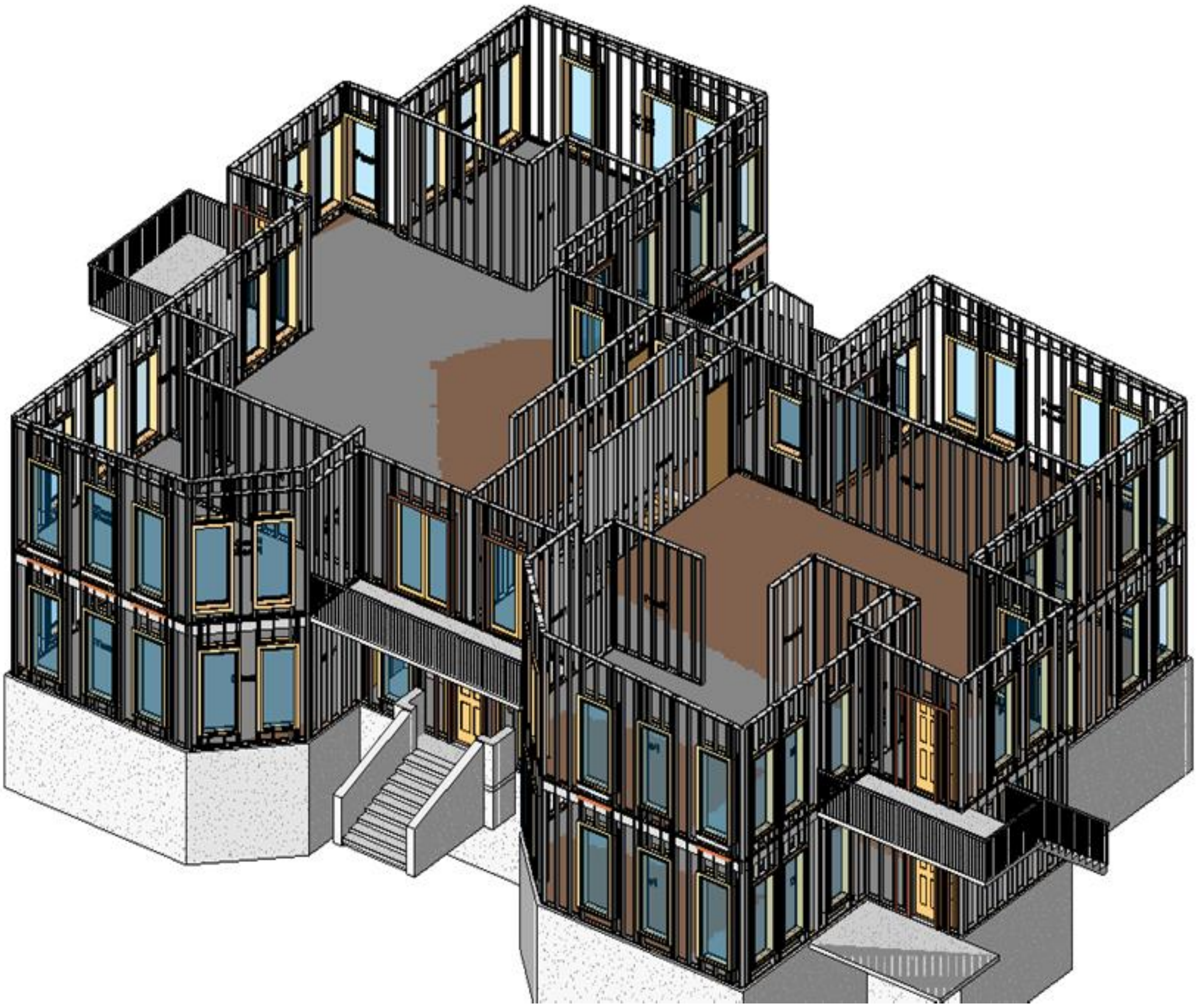

Figure 2. 1: Example of the BIM model (Abu-Hamd, 2015)

2.1.1 Evolution of BIM

BIM gained momentum in the early 2000s through companies like Autodesk and Bentley Systems, primarily targeting cost-effective solutions for large-scale construction projects, including visual and quantitative representations, material procurement, and scheduling. Over time, BIM evolved into a repository of geometric and semantic building information repositories collaboration across design, construction, and operation phases. Digital prototypes facilitate pre-construction testing (Eastman et al., 2008). Initially, BIM faced a slow adoption rate, evolving from manual drafting to CAD and computer-based systems. The building information exchange suffered from inefficiencies, rework, data loss, and falsification due to paper-based methods. BIM revolutionized this by offering end-to-end project support, ensuring a transparent model flow throughout the lifecycle, enhancing efficiency, and promoting information integration among stakeholders. Visualization and simulation capabilities enable aesthetic design, user value interpretation, risk reduction, and comprehensive analysis, covering energy consumption and workflow. (J. Zhang et al., 2022)

2.1.2 BIM Dimensions and LODs

BIM has undergone significant development, encompassing diverse dimensions. These dimensions contain 4D, representing time-related aspects; 5D, which pertains to cost considerations; 6D, which focuses on sustainability and energy performance; and most prominently, 7D, which addresses the realm of facility management. These dimensions add layers of information and functionality to the core BIM model, transforming it into a comprehensive tool for the entire building lifecycle. (Charef et al., 2018) In Figure 2.2, a graphical representation is presented that encapsulates the concept of BIM dimensions, along with associated attributes elucidating the characteristics and functionalities of each dimension.

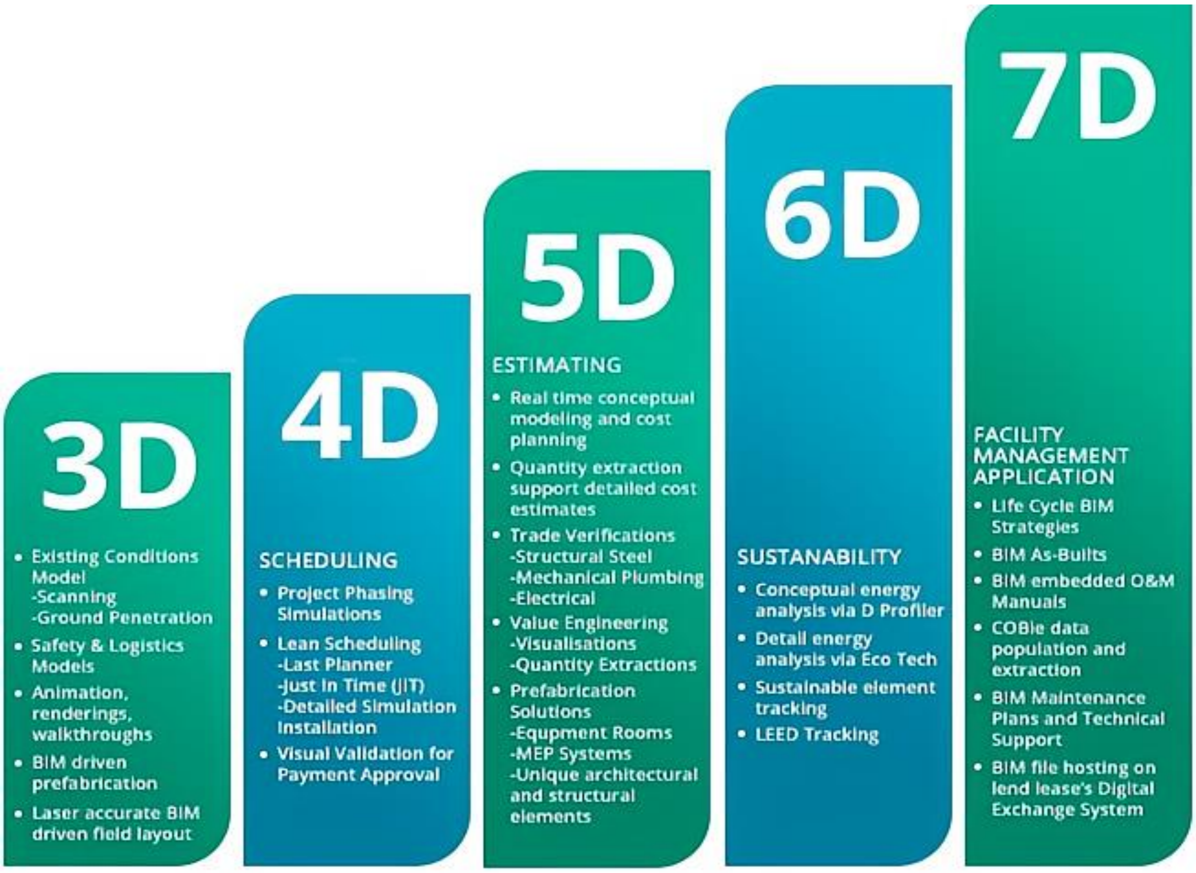
3D
• Existing Conditions Model -Scanning -Ground Penetration
• Safety & Logistics Models
• Animation, renderings, walkthroughs
• BIM driven prefabrication
• Laser accurate BIM driven field layout
4D
SCHEDULING
• Project Phasing Simulations
• Lean Scheduling -Last Planner -Just In Time (JIT) -Detailed Simulation Installation
• Visual Validation for Payment Approval
5D
ESTIMATING
• Real time conceptual modeling and cost planning
• Quantity extraction support detailed cost estimates
• Trade Verifications -Structural Steel -Mechanical Plumbing -Electrical
• Value Engineering -Visualisations -Quantity Extractions
• Prefabrication Solutions -Equpment Rooms -MEP Systems -Unique architectural and structural elements
6D
SUSTANABILITY
• Conceptual energy analysis via D Profiler
• Detail energy analysis via Eco Tech
• Sustainable element tracking
• LEED Tracking
7D
FACILITY MANAGEMENT APPLICATION
• Life Cycle BIM Strategies
• BIM As-Builts
• BIM embedded O&M Manuals
• COBie data population and extraction
• BIM Maintenance Plans and Technical Support
• BIM file hosting on lend lease's Digital Exchange System

Figure 2. 2: BIM dimensions (Max Rodriguez, 2022)

BIM is renowned for its 3D geometric modeling capabilities. The representation of buildings in 3D enables enhanced visualization and spatial analysis. It incorporates a range of elements, including the LOD and the LOG, which play critical roles in the effectiveness of BIM processes through the project life cycle. The LOD reflects the detail and accuracy of the design, materials, components, and systems. The LOD helps to improve collaboration and coordination among different stakeholders and disciplines with a clear understanding of the level of detail and information from the BIM model required. LOD is categorized according to stages ranging from 100 to 500, where the numbers represent a lower to a high level of completeness of the BIM model as it relates to each phase of the Building Lifecycle. The LOD is measured according to LOG and LOI, as shown in Figure 2.3. LOG focuses on the appearance of the objects in a model, while LOI focuses on the properties of the things in a model. (Oliver Eischet, 2023)

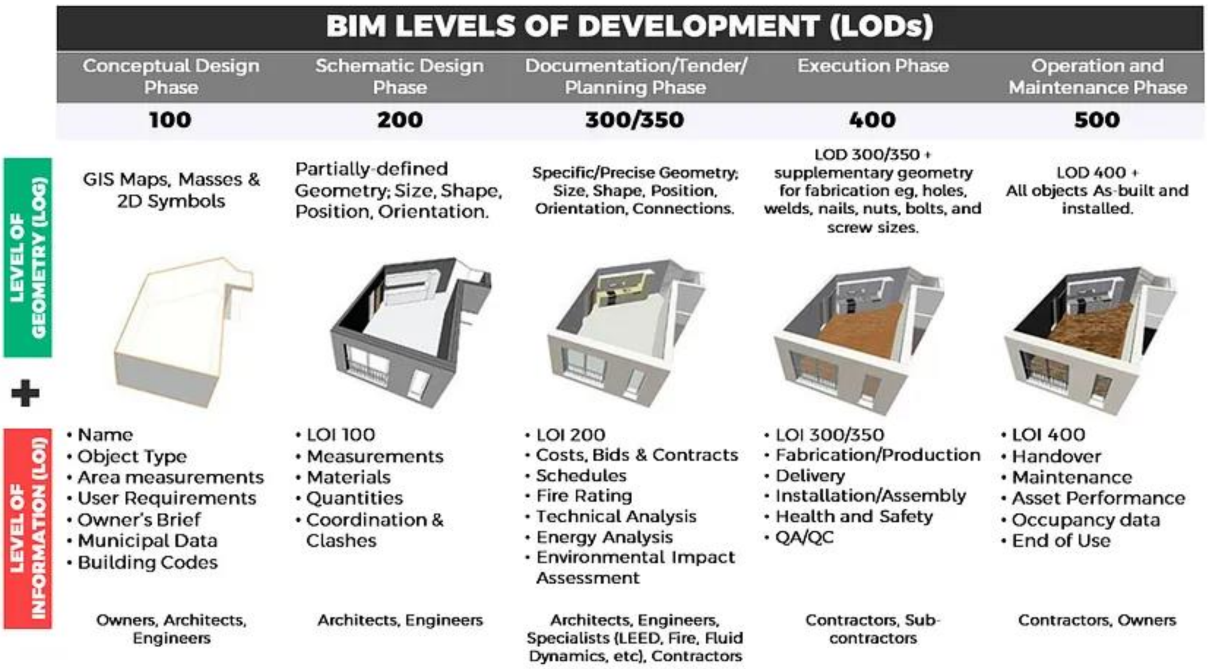

BIM LEVELS OF DEVELOPMENT (LODs)

	Conceptual Design Phase	Schematic Design Phase	Documentation/Tender/ Planning Phase	Execution Phase	Operation and Maintenance Phase
	100	**200**	**300/350**	**400**	**500**
LEVEL OF GEOMETRY (LOG)	GIS Maps, Masses & 2D Symbols	Partially-defined Geometry; Size, Shape, Position, Orientation.	Specific/Precise Geometry; Size, Shape, Position, Orientation, Connections.	LOD 300/350 + supplementary geometry for fabrication eg. holes, welds, nails, nuts, bolts, and screw sizes.	LOD 400 + All objects As-built and installed.
+					
LEVEL OF INFORMATION (LOI)	• Name • Object Type • Area measurements • User Requirements • Owner's Brief • Municipal Data • Building Codes	• LOI 100 • Measurements • Materials • Quantities • Coordination & Clashes	• LOI 200 • Costs, Bids & Contracts • Schedules • Fire Rating • Technical Analysis • Energy Analysis • Environmental Impact Assessment	• LOI 300/350 • Fabrication/Production • Delivery • Installation/Assembly • Health and Safety • QA/QC	• LOI 400 • Handover • Maintenance • Asset Performance • Occupancy data • End of Use
	Owners, Architects, Engineers	Architects, Engineers	Architects, Engineers, Specialists (LEED, Fire, Fluid Dynamics, etc), Contractors	Contractors, Sub-contractors	Contractors, Owners

Figure 2. 3: BIM Levels of development as related to all phases of the building lifecycle (Oliver Eischet, 2023)

2.1.3 BIM and facility management

Effective facility management can help ensure the safety and compliance of the real estate, protect assets, improve employee productivity, and reduce costs. For example, a study conducted by the IFMA found that effective facility management can lead to savings of up to 20% on overall operating costs (Bortoluzzi et al., 2019). The seventh dimension extends BIM into the operational phase. It incorporates real-time data related to facility management, including equipment performance, energy consumption, and occupancy patterns. By connecting IoT devices and sensors, facility managers gain a holistic view of the building's performance. This data-driven approach optimizes maintenance schedules, minimizes downtime, and reduces operational costs. This multidimensional approach aligns with the growing demand for more innovative, efficient, and sustainable built environments. BIM's contribution to facilities extends to lifecycle management, allowing for better decision-making regarding renovations, expansions, or maintenance interventions (Gholizadeh et al., 2018).

2.2 Digital Twin

2.2.1 Digital Twin definition

The term "Digital Twin" encompasses several distinct definitions across various fields of application. One such definition posits that a DT is a realistic representation of a physical object (Wicaksana & Rachman, 2018). Another perspective defines a digital image of a value object, process, or system in the built or natural environment (Bolton A., 2018). Yet another interpretation characterizes a Digital Twin as a true-to-life depiction of the operational dynamics inherent to its physical counterpart. This fidelity is made possible through near real-time synchronization between the digital realm and the physical domain (Schleich et al., 2017).

Notably, utilizing DT should yield tangible benefits, including cost reduction, time savings, and enhanced comprehension of system interrelationships. DTs find applications in many domains, serving diverse purposes such as system analysis, predictive modeling, and support for conservation management efforts. Their versatility extends across various disciplines, encompassing mechanical engineering, aerospace, manufacturing systems, and civil engineering, where their transformative potential is harnessed for manifold objectives (Bolton A., 2018). it furnishes actionable insights that are readily comprehensible and adeptly communicated, thus facilitating the establishment of trust among stakeholders and lending substantial support to the decision-making apparatus. (Akanmu et al., 2021)

DT is a dynamic simulation model that faithfully mirrors the present state of an operational system. It enables a spectrum of functions, including experimentation, in-depth analysis, and effective communication. Consequently, the digital twin framework becomes a conduit for formulating hypothetical scenarios needed to unravel intricate system behaviors and validate outcomes across multiple hierarchical levels (Davila Delgado & Oyedele, 2021).

2.2.2 Integration of DT with different technologies

Numerous studies have been conducted to study the relationship between DT and BIM and are divided into four primary categories. Some researchers have posited the assumption that BIM is a component of DT. BIM is the initial step towards Industry 4.0, encompassing virtual reality and DT. Integrating BIM models into DT information systems can enhance organizational operations. The construction industry uses BIM data to create DT (Gurevich & Sacks, 2020).

In contrast, other researchers consider DT a subset of BIM. They think of DT as a multidimensional digital representation of physical assets that can accelerate BIM's development and benefits in the construction industry (Moretti et al., 2021; Zhao et al., 2021).On the other hand, it is considered that DT is used to map and store component information of existing facilities within BIM, maintaining consistency, (Kaewunruen & Lian, 2019). Some researchers use DT as a synonym for BIM, stating that BIM is, in fact, a form of DT (Sacks et al., 2020), (Twin, 2022). Figure 2.4 illustrates the distribution of researchers based on their varying definitions of the relationship between DT and BIM.

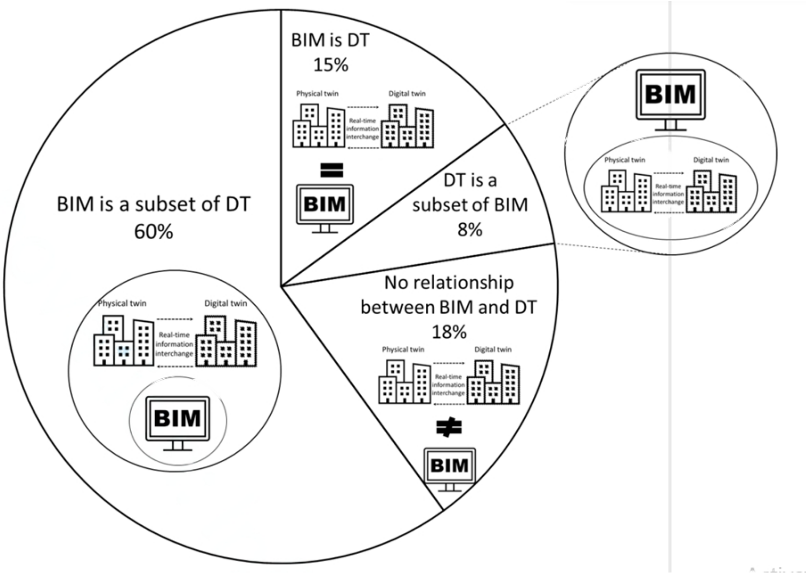

Figure 2. 4: The relationship between DT and BIM (Twin, 2022)

Within the construction domain, the term DT assumes three distinct usages: In the context of the construction industry, DT denotes a genuine representation of structures, processes, or systems. It pertains to a realistic digital portrayal confined within the construction sector. Secondly, DT emerges as an extension of BIM, encompassing data acquisition and processing systems. This interpretation even posits DT as a comprehensive replacement for BIM technology in certain instances. Under this perspective, various DTs are employed for discrete phases of the construction process, suggesting a phased implementation. DT is delineated as a closed-loop digital-physical system designed for the operational management of structures. This conceptualization extends beyond the design and construction phases to encompass constructed assets' ongoing operating life cycle, which will be discussed in more detail. (Boje et al., 2020)

The information mirroring model and later refined as the mirrored spaces model. Until recently, these concepts were collectively referred to as Digital Twins. DT opens fresh perspectives and research avenues for scholars and academics, particularly in areas like integrating BIM and DT for sustainable design and construction (Nguyen & Adhikari, 2023).

Recently, BIM still needs to create intricate digital models encompassing the physical and functional attributes of buildings throughout their visual representation and maintenance (L. Tang et al., 2017). It has emerged as a collaborative approach that fosters efficient communication among various stakeholders involved in the construction process (Bosché et al., 2015). This not only streamlines decision-making but also aids in optimizing building performance. On the other hand, digital twinning involves replicating physical structures in a digital format, enabling real-time monitoring and assessment (Lu & Brilakis, 2019).

Recent advancements have propelled the development of sensors and reality-capturing methodologies, ushering in a new era of precision and accuracy in data collection and representation. This progress has been instrumental in bolstering the capabilities of both BIM and DT technologies (Alizadehsalehi & Yitmen, 2023). Integrating advanced sensors, such as LiDAR and 3D scanners, has facilitated the meticulous capture of building geometry and attributes, creating highly detailed digital replicas. (Kantaros et al., 2023)

2.2.3 Use of DT in the building life cycle

DT has various criteria that are identified for describing and categorizing. These criteria include representation accuracy, creation timeline, potential applications, maturity level, degree of integration, and hierarchy, among others, which serve as distinguishing points. We will focus on the creation of timeline classification. (Gurevich & Sacks, 2020)

DT can be established at various stages in a project's lifecycle. The timing of their development distinguishes them, with early creation being the most efficient, enabling extensive data accumulation. DT is known as DTP when generated before the physical construction phase. This DTP is a prototype of the future real-world object and contains essential information like material quantities, 3D models, and simulation results. DTP’s development begins virtually, facilitating various tests for construction optimization (Michael Grieves and John Vickers, 2017). On the other hand, a DTI is initiated at the outset of production, continuously updated with real-world data after construction concludes, providing an accurate representation of the system's current state and predictive capabilities. The construction industry also employs a hybrid approach, blending elements of DTP and DTI methods. (Gurevich & Sacks, 2020)

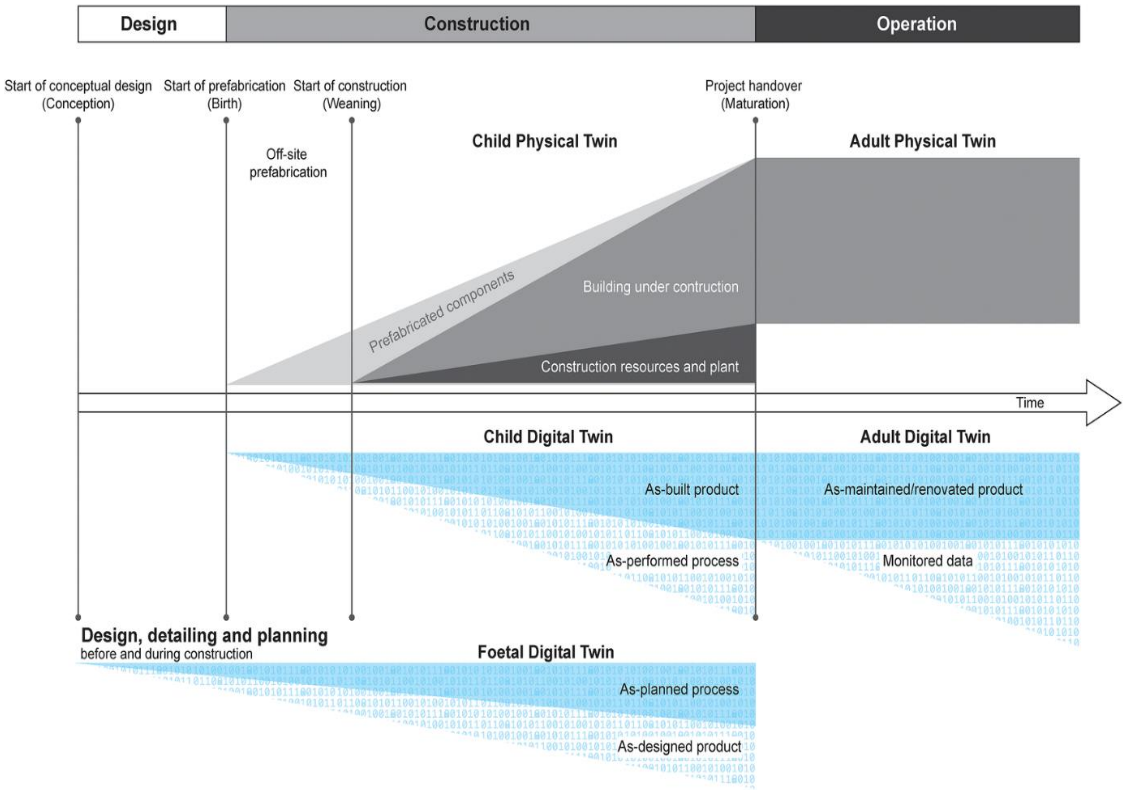
Design
Construction
Operation
Start of conceptual design (Conception)
Start of prefabrication (Birth)
Start of construction (Weaning)
Project handover (Maturation)
Off-site prefabrication
Child Physical Twin
Adult Physical Twin
Prefabricated components
Building under contruction
Construction resources and plant
Time
Child Digital Twin
Adult Digital Twin
As-built product
As-maintained/renovated product
As-performed process
Monitored data
Design, detailing and planning
before and during construction
Foetal Digital Twin
As-planned process
As-designed product

Figure 2. 5: Life cycle of physical and digital building twins (Sacks et al., 2020)

A digital model is crafted according to the client's specifications during the design phase. LOG and LOD of this model progressively increase during the planning phase. Following the analogy of human development stages, this digital model is called a "Foetal Digital Twin" by (Sacks et al., 2020). In this developmental phase, the DT serves as a foundation for simulations and optimizations of the construction process and is denoted as a DTP (Michael Grieves and John Vickers, 2017).

Once construction begins, the physical twin is brought into existence, and its level of detail increases throughout the construction phase. The real-time construction progress is simultaneously reflected in the "Child Digital Twin" through the "As-built product." After construction, the actual system's information content changes minimally, while the digital system continues receiving new data through sensors and state information (Sacks et al., 2020). This continuous enrichment of the DT with sensor data over its lifecycle aligns with the concept of a DTI as described by (Michael Grieves and John Vickers, 2017). Figure 2.5 shows the life cycle of DT in building construction projects.

2.3 Scan-to-BIM

Scan-to-BIM is a transformative process in architecture and construction that involves converting laser-scanned point cloud data into BIM (Andriasyan et al., 2020). The primary purpose of the Scan-to-BIM process is to offer a high degree of accuracy, capturing intricate details of existing structures with precision (Bosché et al., 2015). It facilitates clash detection, helping identify potential conflicts between new and existing building elements (Kor et al., 2023). Scan-to-BIM aids facility managers in efficiently maintaining and managing buildings by offering a comprehensive digital twin (Hosamo et al., 2023).

2.3.1 Point cloud

A widely recognized form of 3D data representation is the point cloud. It is characterized by an ensemble of unstructured points defined by their 3D coordinates (x, y, z). Point clouds portray the occupied space exclusively, leaving unoccupied or undefined space (Bello et al., 2020). Some point clouds include color or intensity information, enhancing visual realism (Tatoglu & Pochiraju, 2012). Point clouds can vary in point density, with denser clouds providing more detailed representations. While the location of sources significantly affects the quality of parts (Xu et al., 2017). Figure 2.6 shows a sample point cloud dataset from building No.1 of the Technical University of Munich.

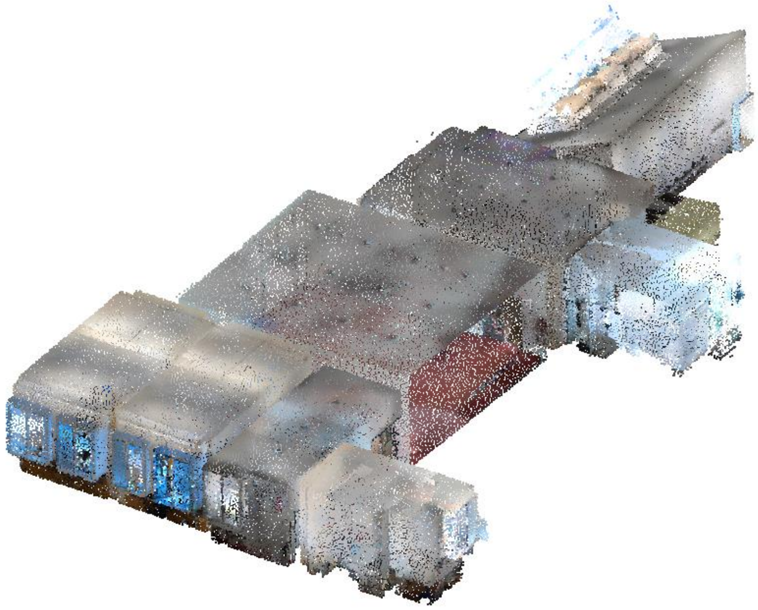

Figure 2. 6: Sample indoor point cloud data.

Point clouds provide exceptionally accurate representations of objects and environments, making them indispensable for tasks requiring precision (Yang et al., 2020), such as the following phases:

- Pre-construction phase: precise as-built documentation from high-density point cloud data provides a detailed view of a location's topography, structures, utilities, and infrastructure. Designers and engineers utilize this data to create plans that seamlessly integrate with existing conditions, reducing conflicts and ensuring project feasibility (P. Tang et al., 2010). Figure 2.7 represents a point cloud dataset depicting an outdoor environment coexisting with a BIM model.
- Design and planning phase: accurate as-built documentation is crucial for design, planning, and immersive 3D visualization. BIM software combines reality capture hardware's point clouds to create precise 3D models. This allows construction professionals to identify issues, make informed decisions, and optimize designs effectively. (Macher et al., 2017).

- Construction phase: Accurate as-built documentation remains crucial. Construction teams can acquire point cloud data to compare with design models at different project stages. This early identification of deviations and conflicts ensures alignment with the design, minimizing costly re-work and ensuring establishing connectivity.

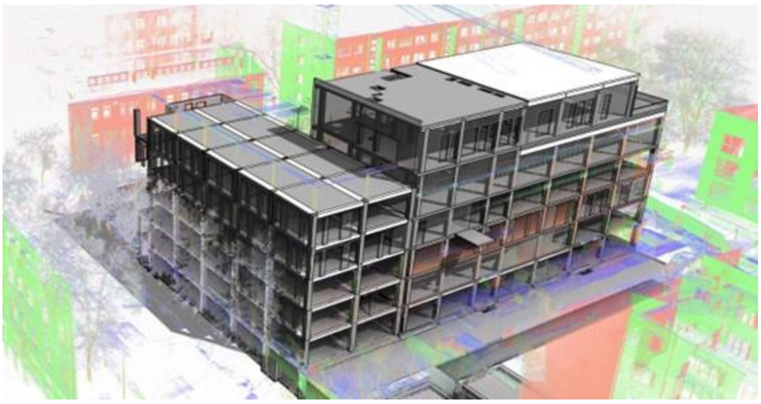

Figure 2. 7: Point cloud of the existing building environment (overlapping with the BIM model)

- As-built phase: The point cloud of the completed project serves as a precise and detailed digital record of the natural world, facilitating as-built documentation and preservation of historical or architectural heritage, creating enhancements, management, and future modifications. Facility managers and owners leverage this documentation to grasp the structure, streamline maintenance, locate specific components, and monitor post-construction changes, ensuring sustained and sustainable use of the facility. (Tsay et al., 2022)

2.3.2 Point cloud acquisition

Over time, advancements and developments in point cloud acquisition techniques such as laser scanning, photogrammetry, and others have refined the generation and utilization of point cloud data (Wang et al., 2018). Numerous methodologies have been developed for the acquisition of point cloud data, for instance:

- Image-derived methodologies directly yield spectral imagery data. This process commences with the acquisition of stereo or multi-view images employing electro-optical systems, such as cameras. Subsequently, 3D point information is computed based on the principles derived from photogrammetry or computer vision theory, either autonomously or in a semi-automated manner. Depending on the distinct platforms involved, stereo and multi-view image-derived systems can be categorized as airborne, spaceborne, UAV-based, or close-range systems. (Javadnejad et al., 2020) In the early stages of aerial traditional photogrammetry, 3D point data were generated with a semi-automated human-computer interaction in digital photogrammetric systems. This approach was characterized by stringent geometric constraints and high survey accuracy but was time-consuming due to manual labor requirements. Consequently, it was not practical to generate dense point datasets over extensive areas. These early image-based point clouds found utility in surveying and remote sensing, particularly in the creation of DSMs and DEMs. (Rakotosaona et al., 2020)

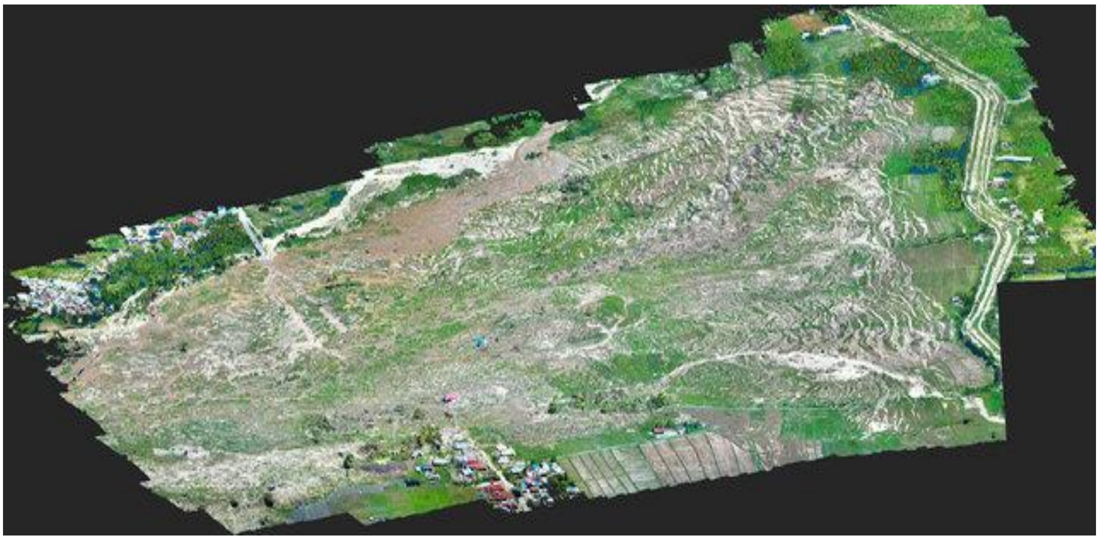

Figure 2. 8: Image-derived point cloud sample (Montgomery et al., 2021)

However, due to limitations in image resolution and the processing capabilities of multi-view images, traditional photogrammetry was constrained to acquiring close to nadir views with a limited representation of building facades from aerial or satellite platforms, leading to the generation of 2.5D point clouds rather than complete 3D models. In specific scenarios, photogrammetry principles could be applied as close-range photogrammetry to obtain points from objects or small-area scenes. However, manual editing was often required at this point of the cloud generation process (Mielcarek et al., 2020).

- LiDAR point cloud generation is a fundamental component of surveying and remote sensing technology. Most LiDAR systems operate on a pulse-based methodology, wherein a laser pulse is emitted, and the time taken for this pulse to traverse the distance to the target is measured. The resultant point cloud exhibits considerable variation in point density or resolution, ranging from less than 10 points per square meter (pts/m2) to many thousands of pts/m2. LiDAR scanning systems are divided into the following methods:

a) Aerial LiDAR system acquired 2.5D point clouds from airborne LiDAR sensors. These point clouds are commonly used in topographic mapping and forestry (Sampath & Shan, 2010).

b) Terrestrial LiDAR captured from stationary terrestrial LiDAR scanners, these point clouds are suitable for indoor and outdoor environments (Heo et al., 2013).

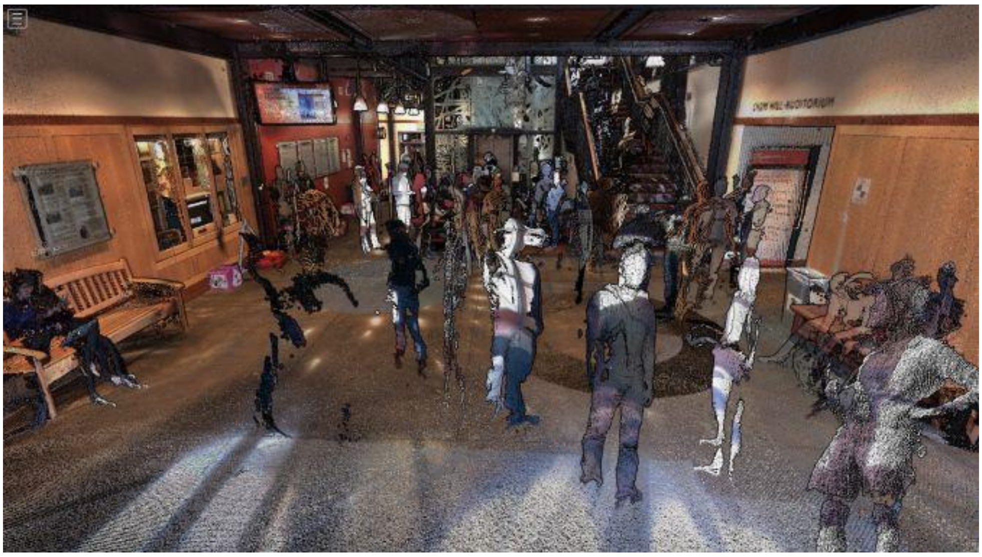

Figure 2. 9: Dense TLS indoor point cloud of a building at Oregon State University (Person et al., 2022)

c) Mobile LiDAR operates from ground vehicles, primarily used for HD mapping (Hackel et al., 2017).

d) Unmanned LiDAR operates from drones collecting dense point clouds, and it is helpful for agriculture and forestry surveying, disaster monitoring, and mining surveying applications (Z. Zhang & Zhu, 2023).

LiDAR is crucial for various applications and has been a primary data source for point cloud research and quality evaluation (Elhashash et al., 2022).

- RGB-D Point Cloud is captured from an RGB-D camera, which is a type of sensor capable of simultaneously capturing RGB color and depth information. Three primary categories of RGB-D sensors exist, each based on different principles such as structured light, stereo vision, and Time-of-flight. Similar to LiDAR systems, an RGB-D camera can measure the distance between the camera and objects, but it does so on a pixel-wise basis. Notably, RGB-D sensors are significantly more cost-effective compared to LiDAR systems (Collings et al., 2015). Within an RGB-D camera, relative orientation parameters among various sensors are calibrated and known, facilitating the synchronized acquisition of RGB images and depth maps. While the point cloud is not a direct output of RGB-D scanning, the known position of the camera's center point enables the straightforward determination of the 3D spatial position of each pixel in a depth map, which can then be directly employed to generate the point cloud. (Cui et al., 2022)

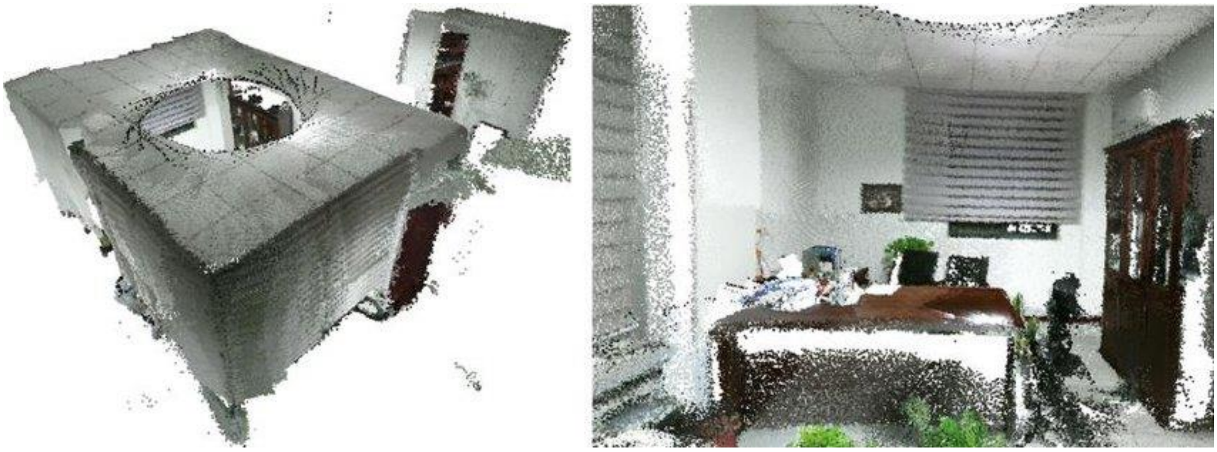

Figure 2. 10: Point cloud captured by RGB-D camera in typical indoor scenes (Chen et al., 2018)

- SAR Point Clouds or Interferometric Synthetic Aperture Radar is a vital remote sensing radar technique that produces maps of surface deformation and digital elevation by comparing multiple SAR image pairs. In recent years, SAR point clouds have gained prominence, opening new possibilities for various applications. Two significant techniques, Synthetic Aperture Radar Tomography, and Persistent Scatterer Interferometry, extend SAR principles into 3D. Synthetic Aperture Radar Tomography excels in detailed urban area reconstruction, while Persistent Scatterer Interferometry achieves denser point clouds comparable to Aerial LiDAR. These point clouds are valuable for urban building reconstruction, offering insight into building facades, temporal deformation, and microwave scattering properties. (Burgmann et al., 2000)

2.3.3 Point cloud preprocessing

The accuracy and completeness of point clouds can be affected by scanning equipment limitations, such as occlusions or environmental conditions. Factors such as obstructions in the scanning path or adverse weather conditions can impede the scanner's ability to capture data accurately. These limitations underscore the importance of considering environmental factors and ensuring unobstructed line-of-sight during scanning processes to attain high-quality point cloud data, which is crucial for various (Abreu et al., 2023). Point clouds can represent irregular shapes and complex geometries with high fidelity, meaning the points are not evenly sampled across the different regions of an object/scene (Bello et al., 2020). Therefore, performing some pre-processing steps on the point cloud data is expected. This may include noise reduction, outlier removal, subsampling, and data alignment to ensure that the point cloud is as clean and accurate as possible (Rakotosaona et al., 2020).

- Outlier Removal methodology used to mitigate noise, filtering, and smoothing methods are applied. Outliers can significantly increase the computational cost of subsequent algorithms, making their removal a crucial preprocessing step. Numerous approaches exist for outlier treatment, broadly categorized as traditional, wavelet-based, and artificial intelligence AI-based methods. Traditional methods encompass distribution-based, depth-based, clustering, distance-based, and density-based techniques, but they struggle with high-dimensional data in sizeable 3D point clouds and real-time constraints (Zaman et al., 2017). Wavelet transformations and AI-based methods serve as alternatives. Wavelet-based methods involve space transformation to identify outliers in non-dense regions. AI methods employ neural networks, support vector machines, and fuzzy logic, offering the advantage of limited a priori assumptions on data. Nonetheless, the challenge of real-time outlier removal in sizeable 3D point clouds remains a concern, especially in AI approaches. (Li et al., 2015)

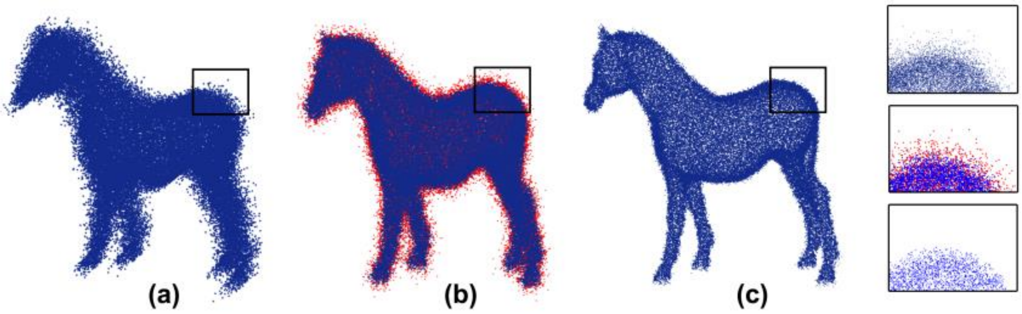

Figure 2. 11: Results of outliers' removal on a horse model: (a) The original point cloud (b) The outliers detected in red color, (c) The resultant point cloud after removing outliers (Zaman et al., 2017)

- Point cloud subsampling is a fundamental process in managing point cloud data, serving to reduce data volume while retaining essential geometric details. This operation is critical for optimizing storage and computational efficiency in applications such as 3D modeling, robotics, and autonomous navigation. Various methods have been developed for point cloud subsampling. One widely used method is voxel grid subsampling, which segments the point cloud into uniform voxels and retains one point per voxel. This technique substantially decreases point cloud density without significant information loss and has been applied in numerous scenarios (Koide et al., 2023). Figure 2.12 shows the difference between an example of a point cloud before and after subsampling.

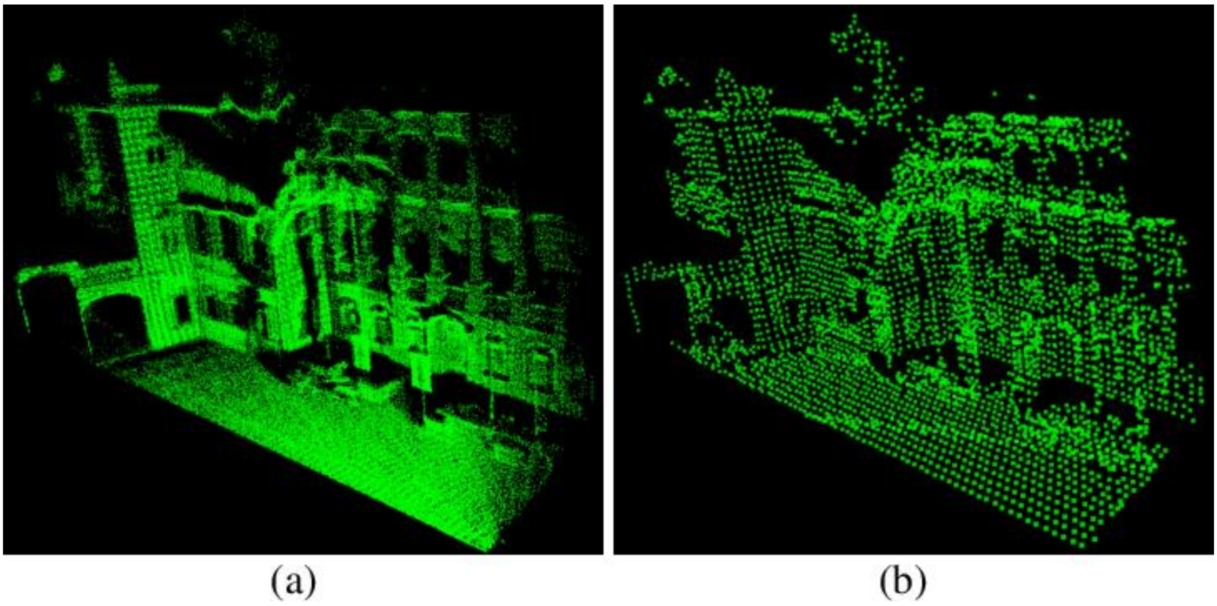
(a) (b)

Figure 2. 12: Point cloud subsampling. (a): the point cloud before subsampling. (b): the point cloud after down-sampling (Cai et al., 2021)

Another approach is random sampling, where points are randomly selected from the original point cloud, and the density of the subsampled point cloud can be adjusted by varying the sampling rate. This technique is simple and computationally efficient, making it suitable for real-time applications. Advanced techniques consider point saliency, such as Poisson disk sampling, which selectively retains points based on their importance to the overall object or scene shape. These methods are beneficial when preserving crucial features and details in the subsampled point cloud is necessary (Hu et al., 2022).

- Point clouds from different sources or scans may not be initially aligned, making it crucial to perform data alignment for coherent modeling or analysis. ICP algorithms

(Besl & McKay, 1992) are widely used for point cloud registration. ICP iteratively refines the transformation parameters to align two or more point clouds, minimizing the overall error.

In accordance with each project's specific requirements, supplementary post-processing procedures on the segmented point clouds are decided.

2.3.4 Point cloud processing

Point cloud processing is a fundamental component of 3D data analysis and interpretation, involving the manipulation, research, and extraction of valuable information from point cloud datasets. Various aspects of point cloud processing include segmentation, feature extraction, registration, classification, object recognition, and modeling.

In the realm of 3D point cloud processing, point segmentation is pivotal in the Scan-to-BIM process. The choice of segmentation criteria and algorithms should align with the specific goals and characteristics of the point cloud data (Varga & Healthineers, 2016). Point cloud segmentation encompasses various methodologies, which can be categorized into both traditional and contemporary AI-based approaches. Traditional techniques include edge-based methods, region growing, and model fitting. An example of a different way for point cloud Segmentation for various building categories is illustrated in Figure 2.13.

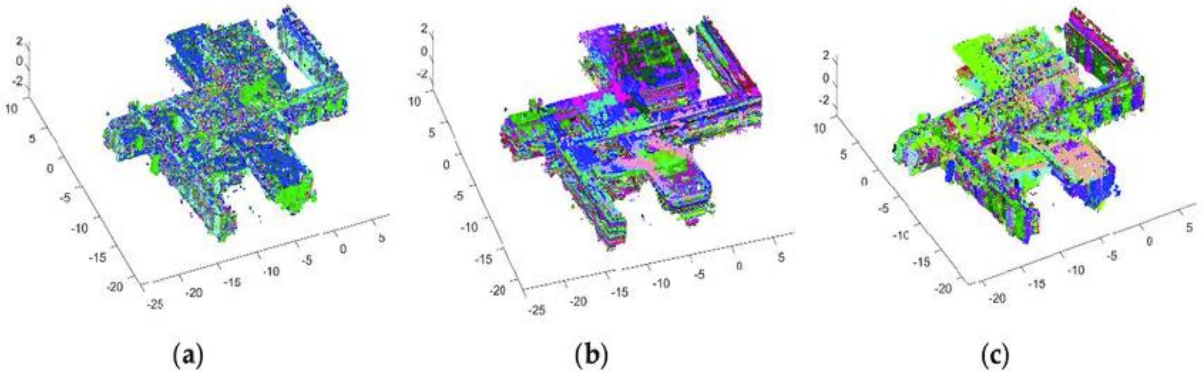

Figure 2. 13 Point cloud segmentation (a) region-based, (b) model-based, (c) hybrid approach. (Shi et al., 2019):

The following techniques can be enumerated for point cloud segmentation:

- Edge-based segmentation method involves the identification of edges within an object, followed by the aggregation of data points located within these delineated edges to assign the object to a defined element, as proposed. (Betsas & Georgopoulos, 2022).

- Region-growing methods initiate their process from one or more initial points, commonly referred to as seed points, which exhibit distinct characteristics of interest. Subsequently, this method expands its influence by iteratively encompassing neighboring points sharing analogous elements, which may contain attributes such as surface orientation, curvature, and others, as described by (Rabbani et al., 2006). Region-based approaches within this framework can be categorically delineated into:
    a) Bottom-up approach: Data-driven techniques are often used while creating a building model using a point cloud dataset through the region-growing segmentation and plan intersection. On the other side, the most problematic points are data density, the quality of the point cloud data can vary depending on the method used to capture it, and data complexity. Point clouds can contain vast amounts of data, making it challenging to extract relevant information efficiently. (Che et al., 2019)
    b) The top-down approach takes a massing or boundary as an input and a series of entities as fillers or targets for insertion. The input design is subdivided based on geometric constraints to assigning spaces. The transformations are done directly on the global boundary conditions, resulting in a solution always conforming to the initial boundary conditions. (Che et al., 2019)
- Model fitting is grounded in the premise that numerous artificially fabricated objects can be deconstructed into fundamental geometric primitives, such as planes, cylinders, and spheres, as illustrated in Figure 2.14 Consequently, these basic shapes are employed in the fitting of point cloud data, and the points that align with the mathematical representation of the respective primitive shape are ascribed to a singular segment. Within the paradigm of model fitting-based categorization, two extensively utilized algorithms include the Hough transform and the RANSAC method. (Buldo et al., 2023)

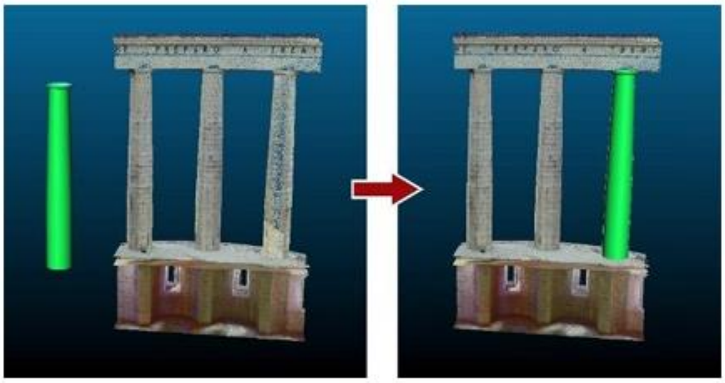

Figure 2. 14: Segmentation of 3D point cloud using geometric primitive fitting (Che et al., 2019)

In recent years, notable advancements in artificial intelligence have revolutionized point cloud processing. Modern AI-driven methods have been developed to achieve tasks such as point cloud classification, semantic segmentation, and object detection. These AI-based approaches have demonstrated significant progress in enhancing the accuracy and efficiency of point cloud segmentation, marking a crucial shift in the field of 3D data analysis. (He et al., 2021)

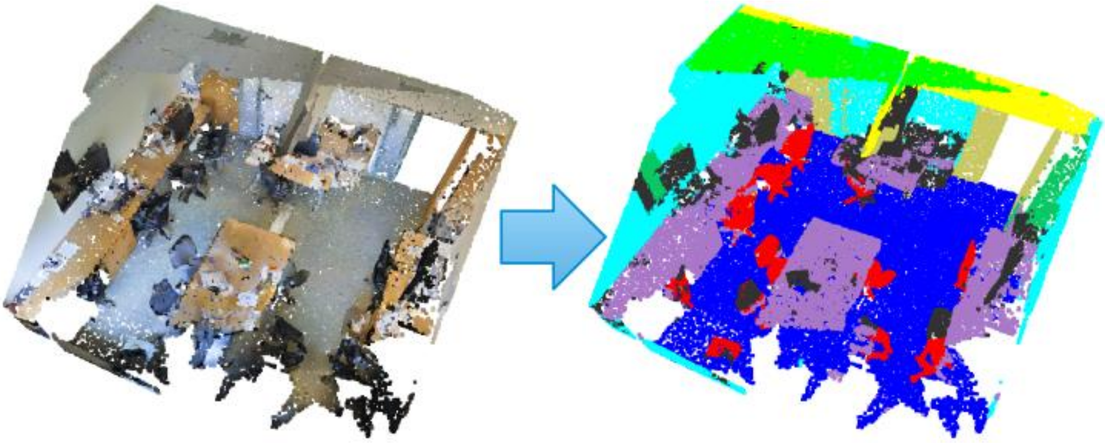

Figure 2. 15: Semantic segmentation of indoor point cloud. (Engelmann et al., 2017)

- Regular supervised machine learning, referring to non-deep supervised learning algorithms. These approaches can be categorized into two main groups: individual point cloud semantic segmentation, which classifies each point or point cluster based solely on its features, and statistical contextual models. (Xie et al., 2020) Individual PCSS methods include classifiers like maximum Likelihood, Support vector machines, AdaBoost, Random Forests, and Bayesian discriminant classifiers (Siemers & Bajorath, 2023). In contrast, statistical contextual models encompass techniques like Conditional Random Fields and Markov Networks, aiming to alleviate noise issues inherent in individual classification. A regularization framework is introduced to address these issues, improving PCSS accuracy. (Niemeyer et al., 2014)

- Deep learning, a rapidly evolving technique in pattern recognition, computer vision, and data analysis, surpasses traditional approaches by utilizing multiple hidden layers to extract high-dimensional features from training data. (Te et al., 2018) While initially applied in 2D computer vision tasks, such as image recognition, object detection, and semantic segmentation, its migration to 3D analysis gained prominence after 2015. (Engelmann et al., 2017) The concept of multiview-based methods and voxel-based 3D CNNs fueled this shift. Point cloud data poses unique challenges due to its unordered nature, necessitating preprocessing transformations. Deep learning-based PCSS methods can be categorized into multiview-based, voxel-based, and point-based, depending on the format of ingested data, such as multiview-based, voxel-based, and directly process point cloud data. (Meng et al., 2019)
- Hybrid segment-wise techniques have garnered attention recently. A hybrid approach typically consists of two key stages: employing an over-segmentation algorithm for initial segmentation and subsequently applying PCSS to the segments generated in the first stage rather than individual points. Pre-segmentation serves a dual purpose in PCSS, reducing data volume and extracting local features. Over-segmentation, a form of pre-segmentation generating super voxels, efficiently reduces data volume with minimal loss in accuracy (J. Zhang et al., 2013). Some PCSS studies also utilize non-semantic PCS methods for pre-segmentation. Deep learning methods incorporate super point structures or supervised algorithms for effective pre-segmentation, exemplifying innovative approaches in point cloud processing. (Landrieu & Boussaha, 2019)

2.3.5 Model reconstruction

The development of point cloud processing methodologies continues to evolve, with a focus on automation and efficiency, mainly through the integration of machine learning techniques. The final step in points cloud processing is identifying and recognizing objects or entities in the point cloud and generating 3D models, including surface reconstructions, BIM, and DEMs. In this context, the following techniques primarily address the indoor building reconstruction domain. This exposition is subsequently enriched with a summarization of supplementary, albeit closely connected, abstraction methodologies and their respective applications.

- Deriving 2D floor plans from 3D point clouds. The approach involves constructing a histogram representing the vertical positions of all measured points within the point cloud data. Okorn observed in this histogram indicated prominent horizontal planar surfaces, specifically the floors and ceilings within the captured space. Subsequently, points associated with these detected flat structures were excluded from consideration (Okorn et al., 2010).

  Following removing such points, linear fittings is performed on the remaining data points. However, it is essential to note that the resulting line segments, which together constituted the floor plan representation, were found to be disjointed and needed to encapsulate complete boundaries of rooms or spaces (Okorn et al., 2010).

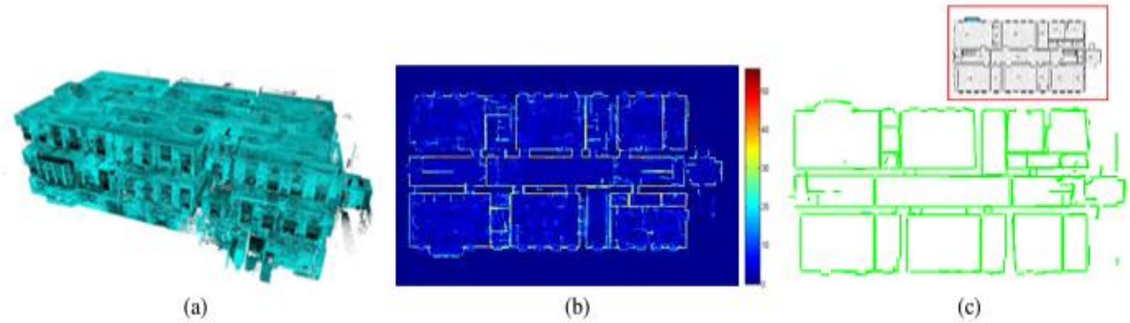

Figure 2. 16: 3D point cloud of a facility (a), histogram Projection (b), resulting 2D floor plan model(c) (Okorn et al., 2010)

- Extracting planar structures about floors, ceilings, and walls through a planar sweep process. This method entails partitioning the XY-plane into piecewise linear segments, followed by classifying these segments into "inside" and "outside" based on the occupancy of cells determined by measured points. Densely occupied cells are designated as "inside," culminating in deriving a 2.5D extrusion representing the room boundary (Budroni & Boehm, 2010).
- Another approach proposes extracting planar structures from point clouds while adhering to regularity constraints. The optimization methodology strikes a balance between data fitting accuracy and the simplicity of the resulting arrangement of planes

(Monszpart et al., 2015). The building's geometry is reconstructed through an inverse CSG approach, which involves the identification of planar structures and their subsequent fitting with cuboid primitives. These primitives are integrated using CSG operations, and the model's quality is assessed using an energy functional. To complete the process, captured images are employed for texturing the resulting mesh model. However, it's important to note that this approach requires the building to be reasonably well approximated by the cuboid primitives, which represents a drawback. (Monszpart et al., 2015)

- Reconstructing planar surfaces encompassing floors, ceilings, and walls within multi-story point clouds. This process begins with detecting modes within a histogram of point height values, enabling the identification of horizontal planes. Subsequently, vertical planes are discerned through the application of the Hough transform. The approach further involves the recovery of occluded segments of the reconstructed surfaces and employs SVM learning for detecting openings. (Adan & Huber, 2011)
- Developing an automated and robust algorithm for partitioning large-scale indoor point clouds into individual spaces has been a longstanding research focus. Previous methods predominantly relied on structural-architectural definitions of buildings, employing various techniques and assumptions for detecting space separators, such as walls. In 3D building modeling, Xiong emphasized using the similarity of planar surfaces for indoor space separation (Xiong et al., 2013). Additionally, It is proposed an iterative clustering algorithm that estimated point affiliations to individual rooms based on visibility probabilities (Ochmann et al., 2016).
  Some researchers sought simplification through tools like RGB image features (Ren et al., 2012) and depth features (Silberman et al., 2012) for identifying planar walls and separating spaces in complex building designs (Ochmann et al., 2016). They introduced an automatic parametric building modeling approach focused on detecting shared wall elements between rooms, as shown in Figure 2.17. Further improvements were made using the RANSAC plane detection algorithm and integer linear optimization to achieve fully automatic room segmentation (Ochmann et al., 2019).

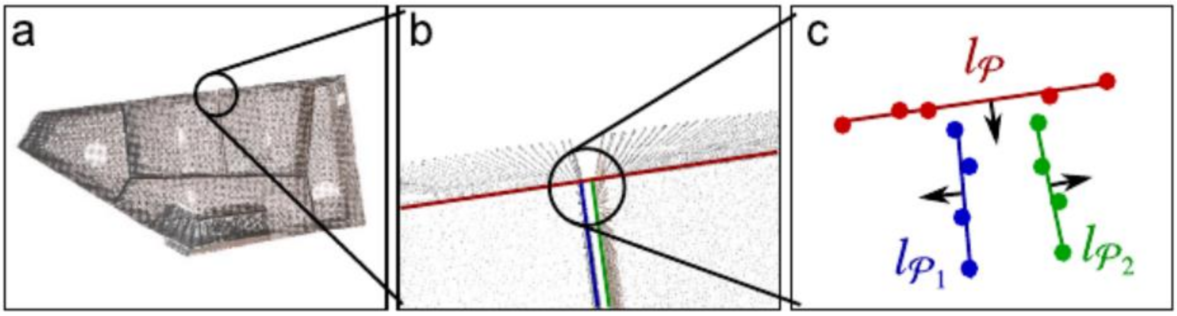

Figure 2. 17: Detecting the parameters of the shared wall between rooms (Ochmann et al., 2019)

A density-based histogram is also developed to analyze and parse 3D space, facilitating the division of indoor point clouds into disjoint areas, thus enabling easy access to information such as space adjacency (Armeni et al., 2016). However, most of these methods required prior knowledge about space layouts or laser scanner locations and were primarily applicable to small-scale environments. Additionally, unsupervised segmentation methods using density-based features often need to be revised related to over-segmentation (Ochmann et al., 2016).

- The delineation and characterization of interior spaces within existing buildings are critical tasks with multifaceted interpretations, dependent on specific applications and purposes (Zlatanova et al., 2020). In the context of 3D model reconstruction and navigation, the demarcation of an enclosed interior space primarily relies on essential structural elements such as floors, ceilings, and walls, which exhibit topological relationships with interconnected spaces (Nikoohemat et al., 2017). Exploring the importance of deducing topological connections among interior spaces, it becomes evident how these insights play a crucial role in achieving accurate geometric modeling of complex areas and simplifying analysis in indoor navigation applications (Zlatanova et al., 2014).

In conjunction with those pioneering efforts and research that mark the foundation theory for automated architectural layout generation from point cloud. This thesis introduces an automatic knowledge-based algorithm that harnesses BIM, DT, Point Cloud, and Scan-to-BIM capabilities and knowledge discussed in this chapter. The focus is on precise region growing segmentation top-down approach space partitioning in diverse real-world indoor environments point cloud to create parameterized BIM Models.

3 Methodology

This chapter presents the proposed framework for creating a parameterized DT model of an indoor environment using point cloud data, as shown in Figure 3.1. The proposed method serves as a strategic guide to effectively tackle the challenges and gaps mentioned in Chapter 2, which aims to bridge the existing gaps and drawbacks by following the Top-Bottom approach inherent in creating parameterized 3D models from indoor point cloud data. The proposed method comprises four primary steps: point cloud data preparation, space placement, setting wall parameters, and refinement. The details of each stage will be elaborated in the following sections. An in-depth analysis of the outcomes stemming from using the envisaged framework will also be presented and thoroughly examined. Dataset 1 shall serve as the primary reference point for most procedural implementations.

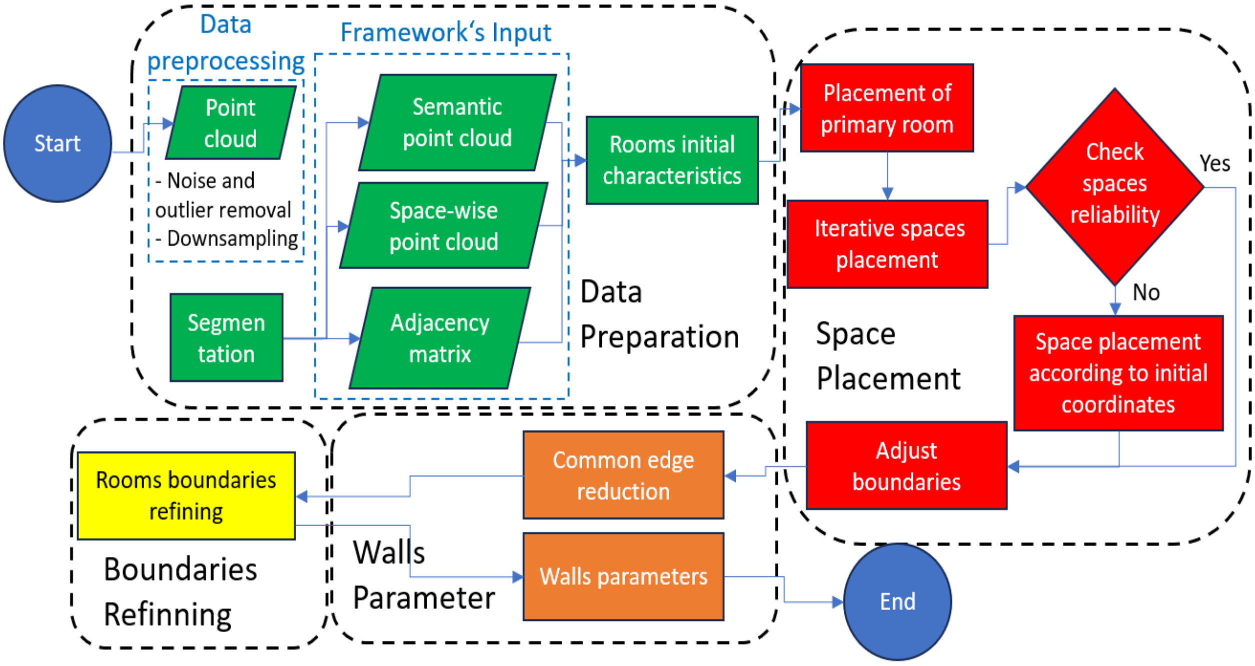

Figure 3. 1: The workflow of the framework

3.1 Data preparation

3.1.1 Data acquisition

A rigorous examination of the methodology mentioned in Figure 3.1 shall be undertaken, focusing on its practical application to various point cloud datasets acquired from the academic institutions of TUM and Stanford University. An in-depth analysis of the outcomes stemming from using the envisaged framework will also be presented and thoroughly examined. Figure 3.2 RGB point clouds of Data Set 1. Dataset 1 shall serve as the primary reference point for most procedural implementations.

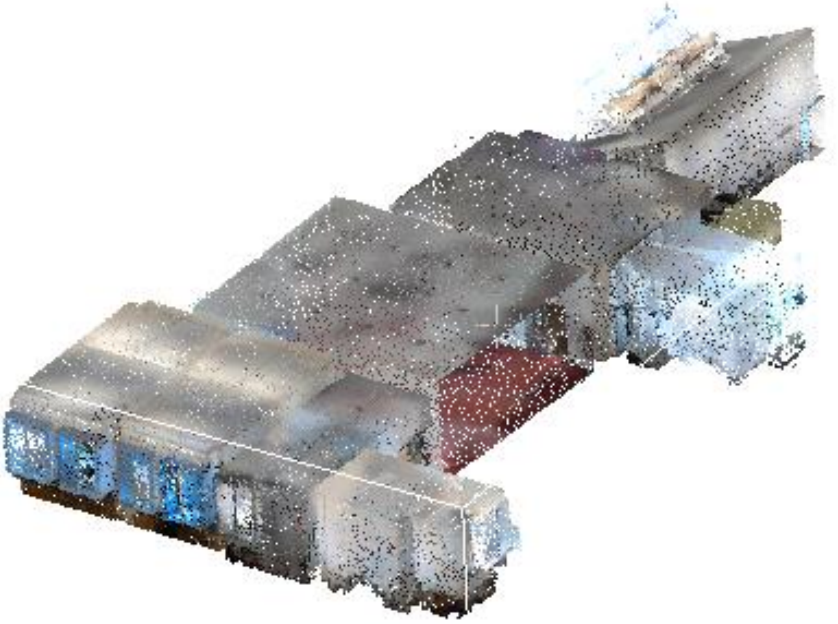

Figure 3. 2: Raw point cloud of Data set 1

3.1.2 Point cloud preprocessing

Point clouds often contain unwanted data points that can distort the accuracy and reliability of 3D models or reconstructions. Noise refers to random, sporadic points introduced by measurement errors or sensor limitations, while outliers are points significantly deviating from the expected model. The provided point cloud should be filtered to eliminate prevalent noise elements, down-sampling, including outlier points removal, and fine-tuning specific details. Scientific methods for noise and outlier removal typically involve statistical analysis, filtering algorithms, and geometric consistency checks. These techniques aim to differentiate genuine data from artifacts, enhancing the precision of point cloud data and making it valuable for further steps. Subsequently, the resolution of the model and scene point clouds is computed, as the key serves as a critical parameter in the registration process. Following this, preprocessing procedures were employed on the provided dataset to curtail the data volume and harmonize the resolutions. The comprehensive elucidation of this subject matter is expounded in its entirety within the confines of Chapter 2.

3.1.3 Point cloud segmentation

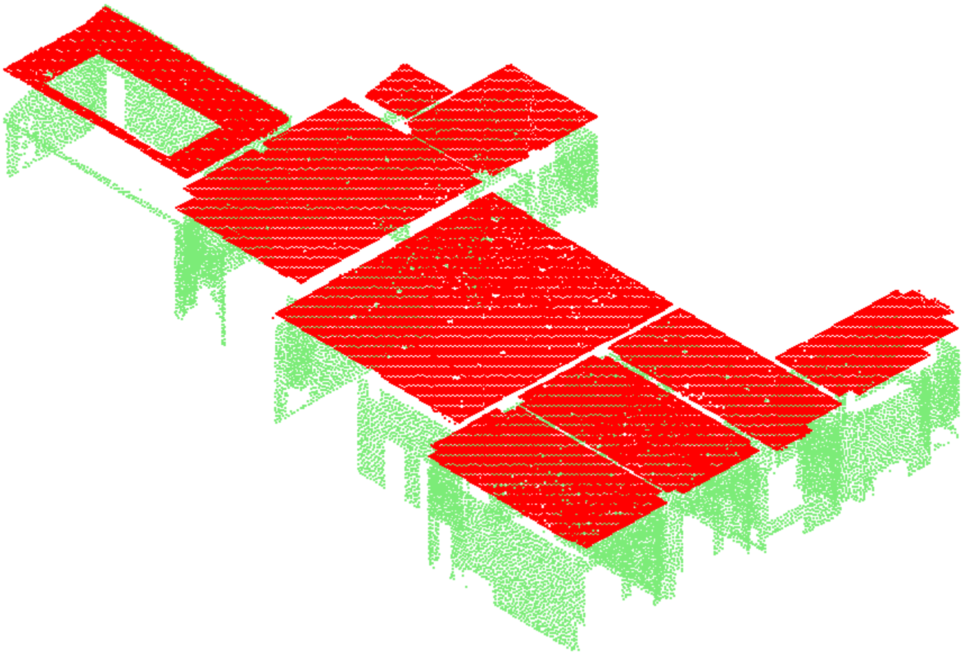

Figure 3. 3: 3D view of ceiling and wall semantic point cloud

semantic segmentation is instrumental in categorizing and understanding the various components within the point cloud data, facilitating subsequent enhanced 3D data analysis by assigning meaning to individual points, enabling object recognition, scene understanding, and improved decision-making. The point cloud data from data set 1 has undergone semantic segmentation using established techniques outlined in Chapter 2. Figure 3.3 illustrates the 3D representation of the resultant semantic ceiling and wall point cloud. Additionally, Table 3.1 provides an example of four points extracted from this point cloud, each assigned a semantic index (0, 1, 2, 3) as indicated. Each semantic index is associated with a specific semantic class, such as ceiling, floors, furniture, and walls.

X	Y	Z	Segmentation Index	Class
19.57049942	5.06750011	2.73000002	0	ceiling
14.41349983	1.26450002	2.71900010	2	furniture
15.73849964	1.26750004	2.72199988	1	floors
13.51636947	3.98419843	2.83166155	3	walls

Table 3. 1: An example of points extracted from semantic point cloud

Dataset 1 has been categorized based on spatial distinctions across the eight discrete spaces according to the placement of the scanning device. Figure 3.4 illustrates the top view of the spaces-wise point cloud for the semantic floor point cloud.

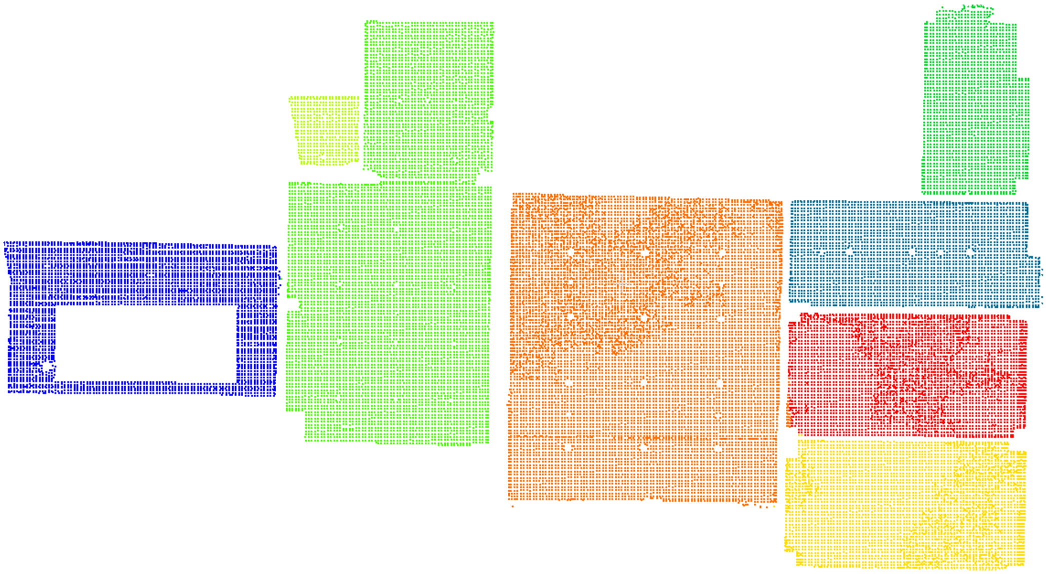

Figure 3. 4: Top view of the space-wise point cloud

Table 3.2 provides an example of three points extracted from the space-wise floor point cloud categorized by the space index.

X	Y	Z	Space Index
19.57049942	5.06750011	2.73000002	4
14.41349983	1.26450002	2.71900010	5
15.73849964	1.26750004	2.72199988	9

Table 3. 2: Three points extracted from space-wise floor point cloud

A space adjacency matrix establishes and elucidates the relationships or connections between distinct rooms or areas. This matrix presents a structured representation of how the rooms are interconnected, serving as a visual aid in comprehending the spatial organization within the project. A space adjacency matrix often represents binary spatial relationships between elements, such as rooms, spaces, or regions in a layout or network. In this binary representation, a "1" in the matrix indicates adjacency (i.e., two spaces are adjacent), and a "0" shows non-adjacency (i.e., two areas are not contiguous). Table 3.3 presents the adjacency matrix representing the spatial relationships among eight distinct spatial entities delineated in Data Set 1.

Rooms	**Room 1**	**Room 2**	**Room 3**	**Room 4**	**Room 5**	**Room 6**	**Room 7**	**Room 8**
Room 1	0	0	0	1	0	0	0	0
Room 2	0	0	1	0	0	0	1	1
Room 3	0	1	0	0	0	0	0	0
Room 4	1	0	0	0	1	0	1	0
Room 5	0	0	0	1	0	0	0	0
Room 6	0	0	0	0	0	0	1	1
Room 7	0	1	0	1	0	1	0	1
Room 8	0	1	0	0	0	1	1	0

Table 3. 3: Adjacency matrix

3.1.4 Rooms initial characteristics

The rooms initial characteristics are created through a computational process involving the determination of the maximum X value minus the minimum X value across all data points comprising the spatial point cloud to derive the width, and likewise, the maximum Y value minus the minimum Y value to establish the length of the spatial domain. The derivation of the bottom-left coordinate entails the identification of the data point characterized by the minimum X and minimum Y values. Concurrently, the computation of the number of neighboring points is derived by an adjacency matrix.

By applying this methodology, the examination of segmented floor points of data set 1, comprising diverse spatial elements across eight floors within a point cloud dataset, is undertaken. The primary objective of this analysis is to ascertain the dimensions of bounding boxes enclosing individual rooms, determine the bottom-left coordinates, and quantify the number of neighboring rooms, as presented in Table 3.4.

Room ID	Length	Width	Bottom Left Coordinate (x,y,z)	Number of adjacent spaces
1	28.62	16.06	(-43.13, -178.14, 0)	1
2	26.16	11.07	(38.36, -169.22, 0)	3
3	11.05	19.55	(52.18, -157.46, 0)	1
4	22.03	44.04	(-14.35, -183.33, 0)	3
7	29.34	32.61	(-9.06, -189.91, 0)	4
5	7.08	7.02	(-13.43, -154.16, 0)	1
6	26.03	14	(36.72, -196.4, 0)	2
8	24.69	12.88	(38.22, -182.69, 0)	3

Table 3. 4: Rooms characteristics

3.2 Spaces placement

3.2.1 Placement of the primary room

The predominant geometric characteristic of rooms or spaces within a building often conforms to a rectangular shape. This prevalent geometric simplicity renders rectangles suitable approximations for modeling purposes in many cases. (Mura et al., 2016)

A more systematic approach entails initiating the placement process by considering spaces with larger areas or those exhibiting more substantial interconnections with adjacent rooms. This strategy facilitates their placement based on their respective spatial coordinates. Subsequently, adjacent spaces of the primary can be arranged in relation to the primary room. In this proposed framework, the selection of the primary room should be prioritized by the highest number of adjacent spaces, as indicated in the room's characteristics table. Employing this principle and referencing table 3.4, the primary room is identified as the room of ID 7, having four adjacent spaces. The primary room should be positioned in accordance with the specified bottom-left coordinates and dimensions found in the table. When this approach is applied to data set 1, Figure 3.5 provides a visual representation of the primary spatial room's placement within the context of its point cloud.

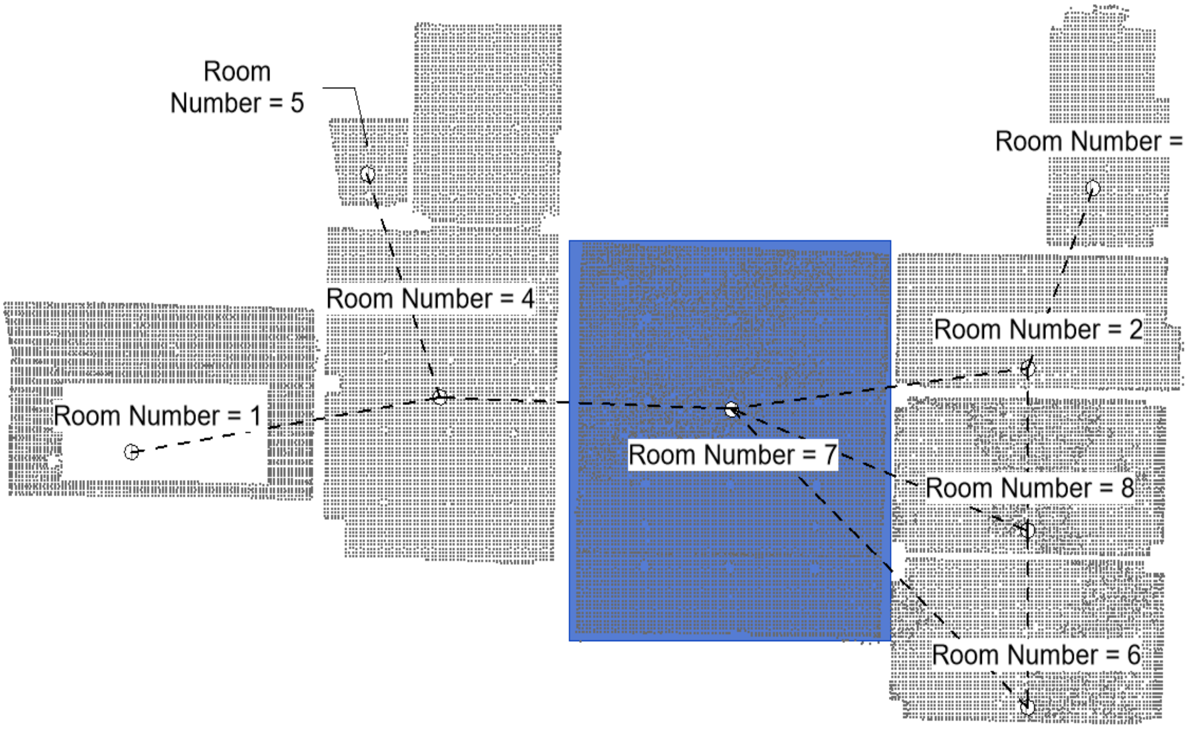

Figure 3. 5: Data set 1 – Rooms Characteristics

3.2.2 Iterative placement of the adjacent spaces

In the process of positioning adjacency spaces or rooms, an iterative approach is employed. The adjacent space is systematically placed around the perimeter of the primary room with specific spacing (d1), and the number of points of spaces-wise point cloud inside corresponding to the same adjacent space's bounding box in each placement is counted and stored. After all iterations, the trail with the highest points count is identified and labeled as the "Adjacent room's trail has the highest number of points," as shown in Figure 3.6. Then comes the second series of iterations by the placement of the adjacent room's bounding box along the path between the bounding boxes, have an index of (Adjacent room's trail o highest number of points) +1 and index of (Adjacent room’s trail o highest number of points) -1 from first series of trails but with a smaller value of spacing (d2) as shown in Figure 3.7. Implementing this approach showed Figure 3.6 and Figure 3.7 yields accurate results while significantly reducing computational time, as it filters the number of points within the spaces effectively.

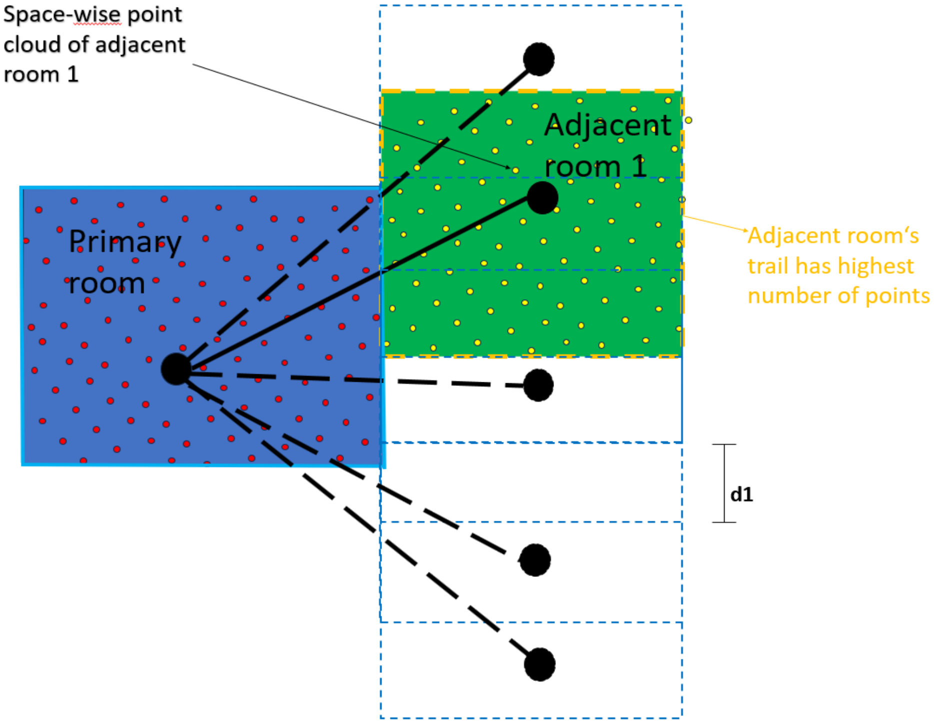
Space-wise point cloud of adjacent room 1
Adjacent room 1
Primary room
Adjacent room‘s trail has highest number of points
d1

Figure 3. 6: Procedure of space alignment – first series of iteration

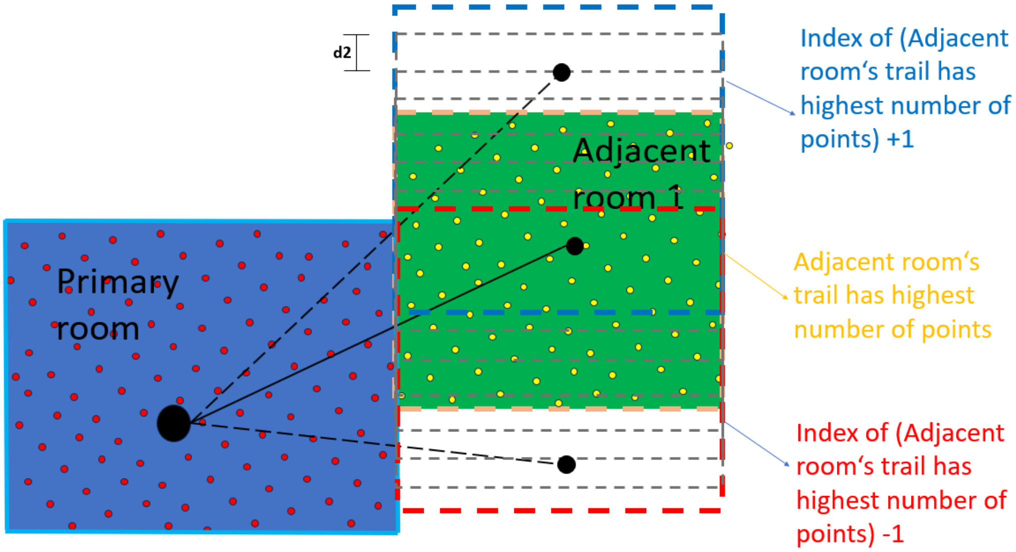
d2
Adjacent room 1
Primary room
Index of (Adjacent room‘s trail has highest number of points) +1
Adjacent room‘s trail has highest number of points
Index of (Adjacent room‘s trail has highest number of points) -1

Figure 3. 7: Procedure of space alignment – second series of iteration

Subsequently, the same iterative process should be applied to each room derived from the initially created spaces. However, it is imperative to exclude any connections between rooms that have already been made. While implementing the previous algorithm, the applied values of d1 and d2 are 30.48 cm (1 ft) and 7.62 cm (0.25 ft), respectively. Figure 3.8 illustrates the bounding boxes' final arrangement of adjacent rooms surrounding the primary room implemented on data set 1, with alignment along its boundary.

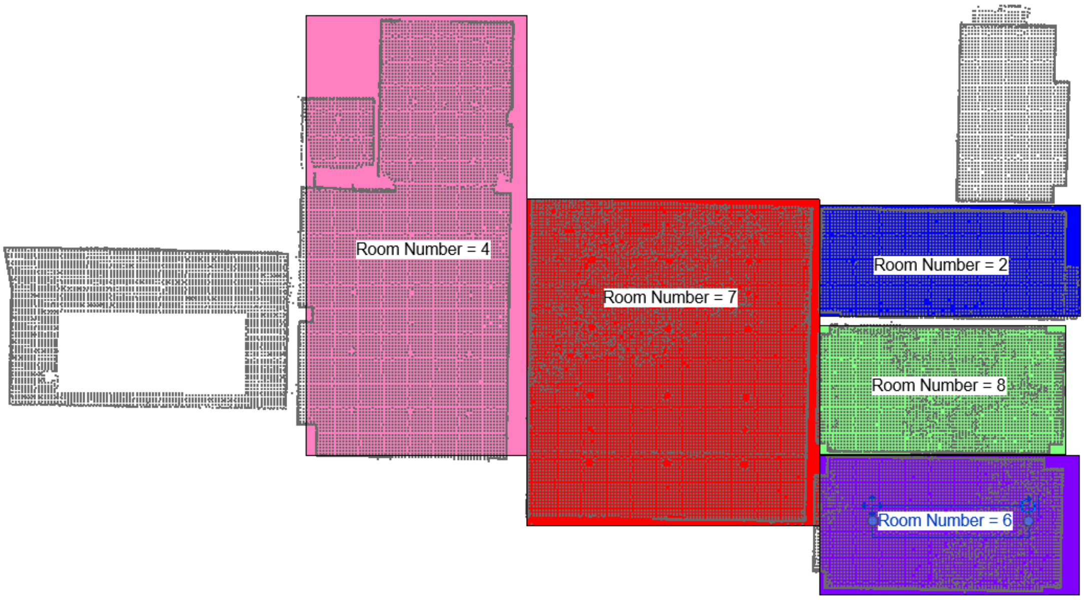

Figure 3. 8: Adjacent spaces around the primary room

Upon completing the placement of adjacent rooms for the primary space, an identical procedure will be implemented for all the newly generated rooms to arrange their respective adjacent spaces. The rooms already in existence are excluded to prevent any instances of overlapping.

3.2.3 Check the reliability of spaces

An additional verification step during room placement, as shown in Figure 3.1, is required to assess the ratio of points positioned within the modeled space to the total points defined in the space-specific point cloud. This ratio, denoted as the "Reliability factor, " is subsequently compared to the allowable reliability factor.

$$Reliability\ factor = \frac{Counted\ points\ inside\ the\ space}{Total\ number\ of\ points\ defined\ in\ spatial\ point\ cloud}$$
$$\geq User\ defined\ allowable\ reliability\ ratio$$

If the reliability space factor exceeds the user-defined allowable reliability threshold, the placement of space is considered successful. Conversely, if it does not meet this criterion, the space must be relocated to the bottom left coordinates previously defined in Table 3.1.

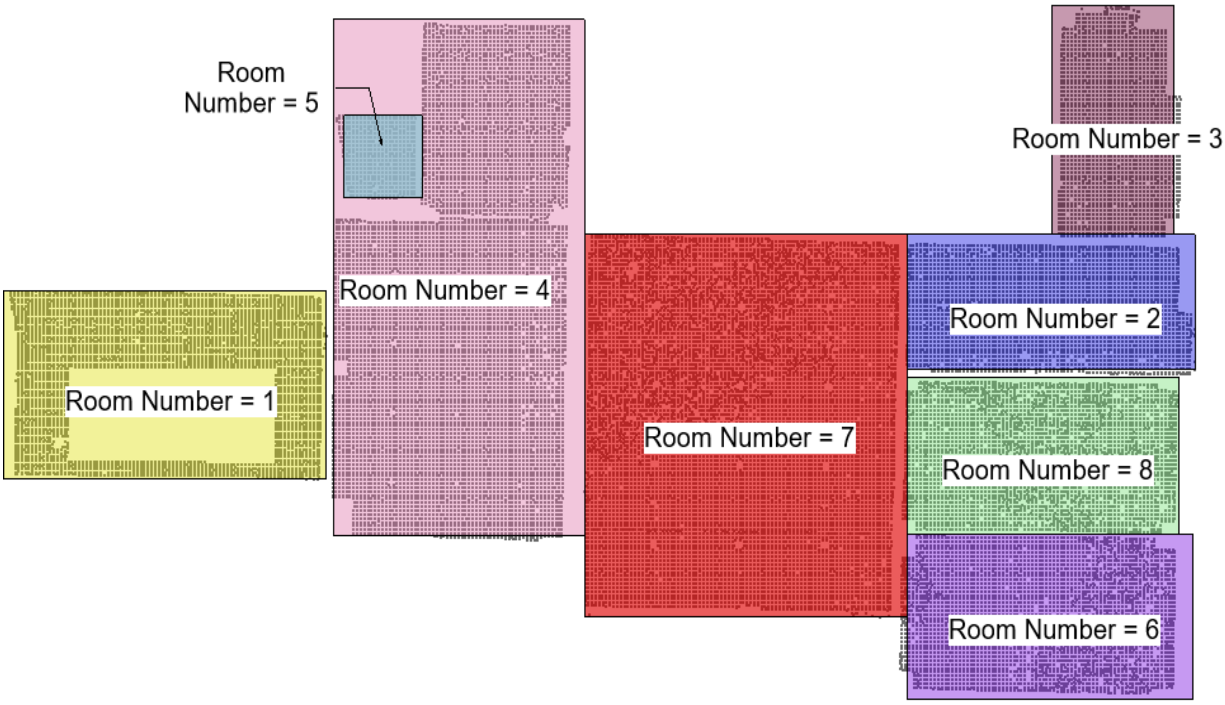

Figure 3. 9: Check the reliability of space placement

A critical verification step ensures the reliability of bounding box positioning, assessing the ratio of points inside the box to the total number of points within the room. Figure 3.9 illustrates the results of the execution of the iterative placement of adjacent spaces algorithm discussed in section 3.2.2 on data set 1, incorporating the evaluation of space placement reliability with a user-defined allowable reliability ratio of 95%.

3.2.4 Adjust spaces' boundaries

Establishing connectivity between the disconnected spaces' boundaries is necessary before proceeding in extracting boundaries parameters. To address spatial disconnections arising from their non-interconnection as initially defined in the adjacency matrix. To resolve such instances, the joint edge of adjacent spaces repositioned in the middle between the disjoint rooms as elaborated in Figure 3.10 or illustrating sample.

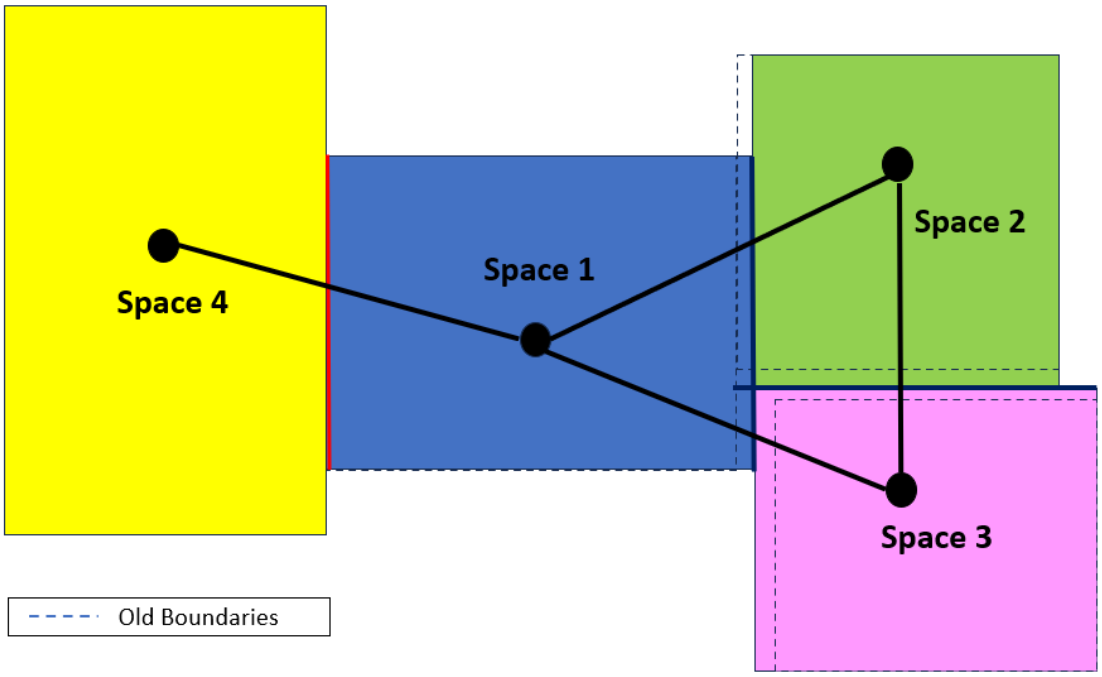

Figure 3. 10: Adjustment of spaces’ boundaries

3.3 Boundary parameters

3.3.1 Merging common walls

To model the wall or space edges effectively, it is imperative to address the issue of edge overlap, aiming to create a unified edge that can subsequently serve as a basis for modeling the walls. This conflict solution involves identifying individual edges, which are parallel in direction and with a specific range of width as distinct walls. To tackle this challenge, a computational approach is employed. A loop is implemented to iterate through each potential edge merger candidate, systematically checking for edges with the same orientation and within a specified distance tolerance. If those common edges are found, an attempt is made to merge them into a single line, as illustrated in Figure 3.6. The detailed code used in this algorithm is provided in Appendix A.1.2 for reference. While implementing this approach of delineation of spaces and boundaries for data set 1, a tolerance of 50 cm for shared edges is assumed.

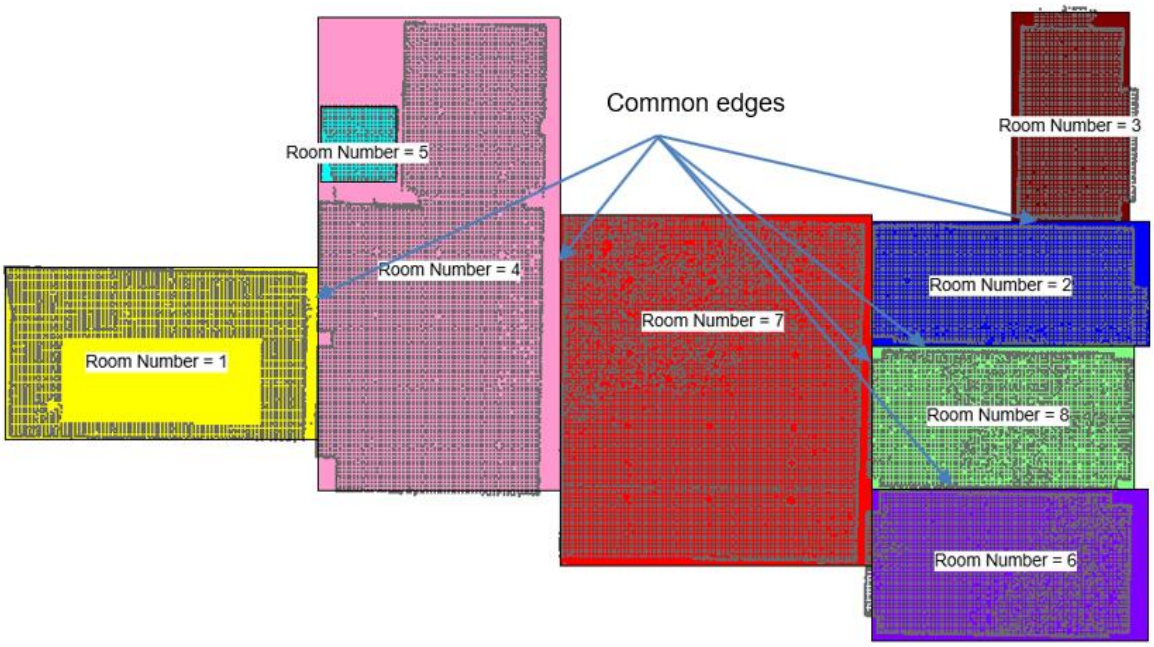

Figure 3. 11: Merging the common walls

3.3.2 Refinning the boundaries of spaces

Given that not all spaces or rooms may possess a rectangular shape, it is imperative to undertake a refinement of their boundary delineations. Subsequently, the entire spatial area is subdivided into smaller units, each separated by initial distance, and an approximation of the number of spaces is made. Then, the total length or width of the spatial area is then proportionally distributed over these approximated spaces, as shown in Figure 3.12. An assessment is subsequently conducted to identify rectangular areas that either lack any data points or contain a percentage of points defined in the semantic floor point cloud falling below a predetermined threshold. These identified rectangles and their respective boundaries are subsequently subtracted from the overall spatial area, resulting in the creation of new spaces with modified boundaries.

While implementing the same approach on data set 1, the determination of the initial dimension has been derived empirically to be 2 meters through an iterative process aimed at identifying the most suitable value. It is essential to emphasize that reducing the number of smaller rectangles into which a room is divided will inevitably result in increased computational time.

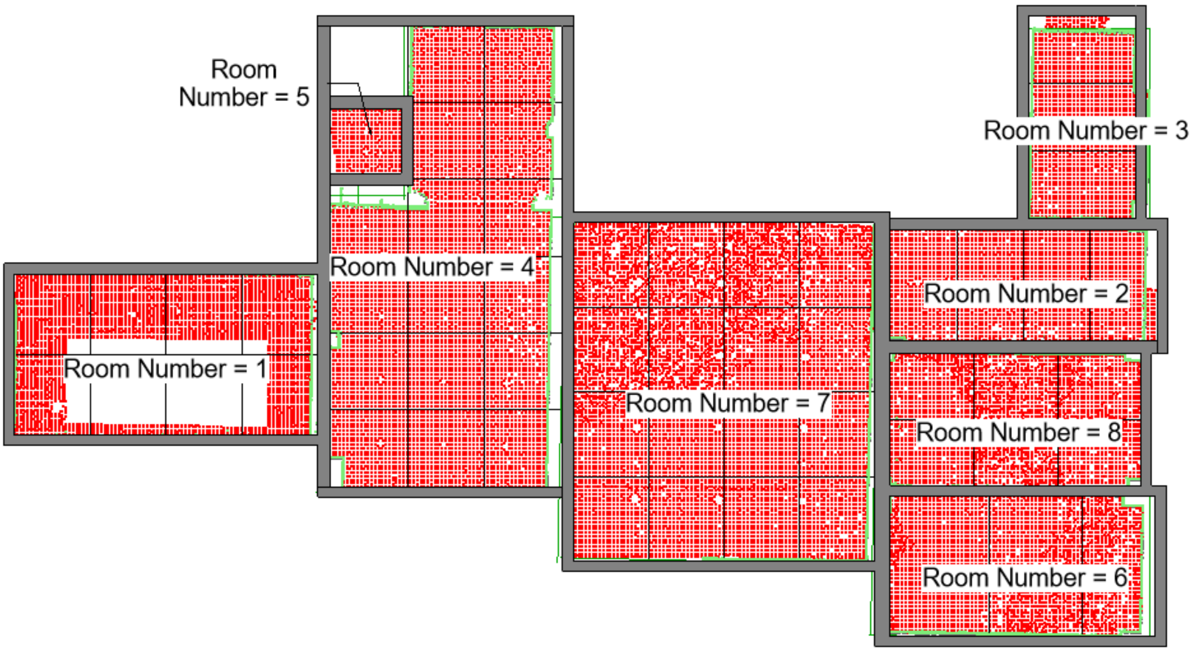

Figure 3. 12: Refinning the boundaries of spaces

In Figure 3.12, it is evident that the rectangular area situated in the top-left corner of room 4 does not contain any points within its confines. Consequently, this rectangle is deemed ineligible for inclusion. Therefore, a revision is necessitated, involving the re-drawing of the boundary for room 4.

This redrawing operation results in an overlap occurring between the upper boundary of Room 4 and the corresponding boundary line of Room 5. To rectify this conflict, two potential strategies may be employed. The first entails manual intervention within the Revit software, wherein the overlapped walls are deleted during the creation process. The second strategy involves the implementation of an overlapping boundary algorithm once more, with the objective of autonomously resolving this overlap issue.

3.3.3 Extraction of wall parameters

Specific prerequisites have already been found in the preceding phases to establish the dimensions of the walls. To ascertain the wall thickness, the walls generated along the boundaries of the rooms have been classified into two distinct types. The first type contains the common borders between rooms or internal walls, and the second type is the barriers found in one room only. For the first category, the semantic wall point cloud is employed. This involves filtering the points corresponding to edges or walls by encapsulating them within bounding boxes, each corresponding to an edge from the previously generated list of merged edges in step 3.3.1. Only the points located within these bounding boxes are considered for further analysis. Subsequently, the average distance of all points to the center line of the wall within its bounding box is computed, and this value is then multiplied by 2 to determine the width of the respective walls.

$$Wall\ Width = (\frac{1}{n}\sum_{i=1}^{n} di) * 2$$

di = the distance between the point to the corresponding planned point on the wall centerline

n = Total number of points inside the bounding box

Regarding wall height, it is also determined using the bounding box approach. This entails calculating the difference between the maximum Z value among the segmented points enclosed within each bounding box and the minimum Z value within the same bounding box.

While implementing this approach on data set 1, the minimum and maximum values for common wall thickness are assumed to be 300 mm and 600 mm, respectively. Furthermore, increments in wall width are restricted to 50 mm intervals. It is important to emphasize that, to ensure the algorithm's error-free operation, wall families corresponding to the specified wall dimensions must be preloaded into the Revit model prior to its execution. Appendix A1.3 shows the algorithm used for finding Internal wall width.

Also, the second category of walls comprises what is referred to as "outside walls," which are postulated to possess a uniform width of 300 mm throughout their extent.

In consideration of wall height determination, as previously elucidated, it is imperative to adhere to specific calculations. However, it is noteworthy that the minimum allowable wall height should be established at 3000 mm. Subsequently, any incremental adjustment should be carried out at intervals of 100 mm, aligning with the approximate value of the disparity between the highest and lowest points identified within the segmented wall point cloud data encompassed within the expanded bounding box associated with the respective wall. This approach ensures a precise and contextually relevant determination of wall height that accounts for the nuanced variations within the observed wall geometry.

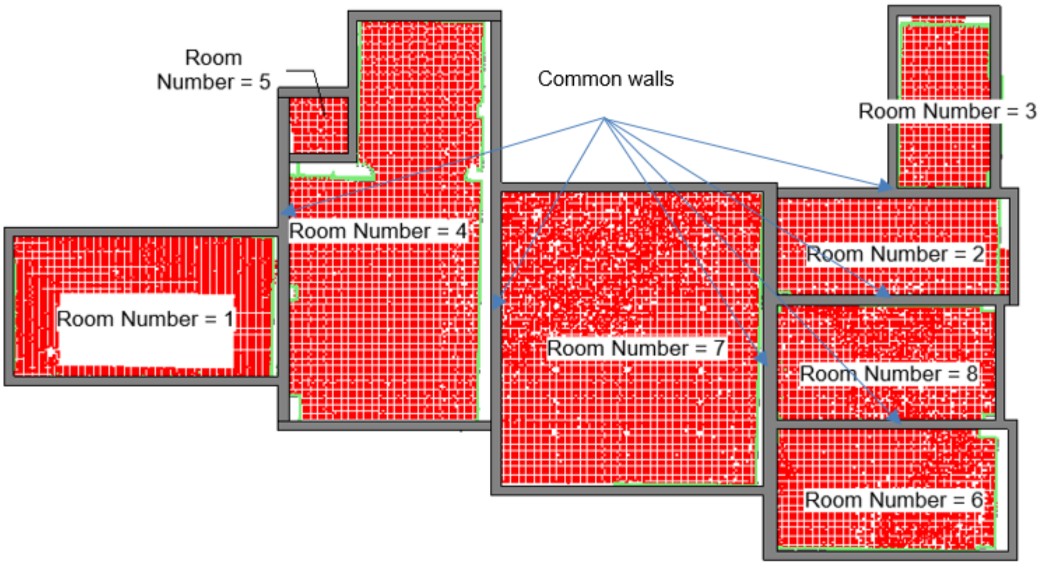

Figure 3. 13: Top view of reconstructed BIM model

3.4 Summary

An essential primary objective during framework development is the minimization of iterations over the points to enhance computational efficiency. Additionally, various tools are employed for testing and refining the framework. These tools include Autodesk Revit as geometry generation and modeling program. Revit's comprehensive capabilities align closely with the framework's needs, excelling in managing complex spatial representations and parametric relationships. Its integration with the Revit API is crucial, allowing custom applications to translate indoor data into parameter-based models. The API enables the integration of custom algorithms, making it a robust platform for synthesizing indoor environment data into models. The framework is encapsulated within a dedicated tool accessible within Revit, facilitating analysis and modeling tasks. The automated procedural framework is implemented in the C# programming language because it can minimize execution time. This framework is integrated into the Revit environment by incorporating the respective dynamic link library (.dll) into the existing set of Revit .dll files. Upon successful integration, the resultant add-in becomes accessible within the Revit interface.

4 Results

In this section, we present an analysis of the outcomes obtained by applying the proposed reconstruction framework, as delineated in Chapter 3. The methodology has been tested and validated on four distinct datasets of point clouds acquired from the academic institutions of TUM and Stanford University.

4.1 Inputs

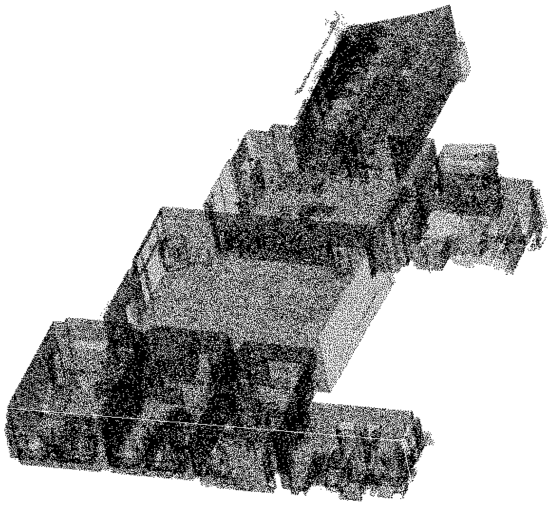

Figure 4. 1: Raw point cloud of data set 1

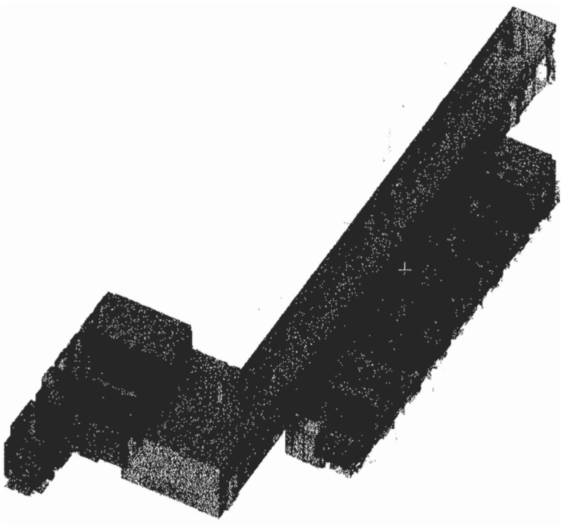

Figure 4. 2: Raw point cloud of data set 2

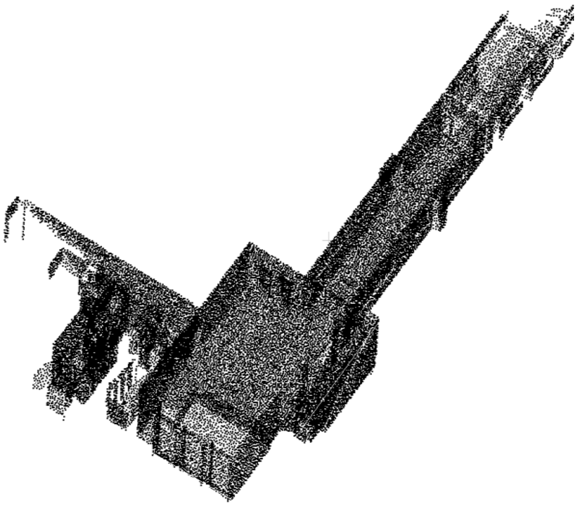

Figure 4. 3: Raw point cloud of data set 3

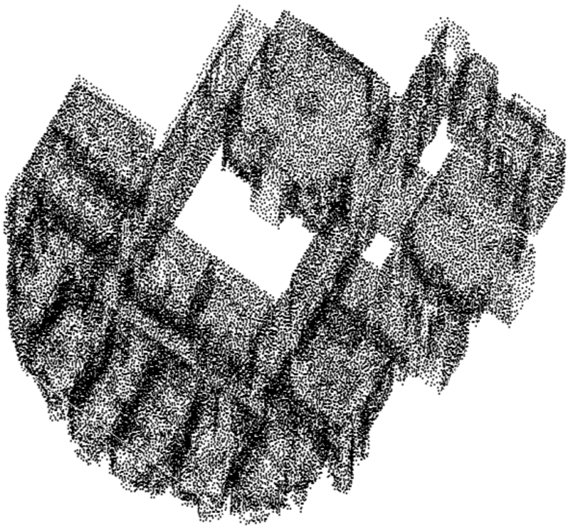

Figure 4. 4: Raw point cloud of data set 4

Figures 4.1, 4.2, 4.3, and 4.4 provide visual representations of the unprocessed point clouds for the four distinct datasets. Additionally, Table 4.1 presents essential quantitative information for each dataset, including the number of rooms, the point count for the semantic floor and wall point clouds, and the total length and width for each point cloud. Furthermore, the table offers an assessment of the point cloud quality through optical visualization.

Data sets	No. of rooms	PC Quality	Number of points – wall PC	Number of points – floor PC	Length (m)	Width (m)
Data set 1	8	9	32001	361640	32.8	17.9
Data set 2	12	8	64033	66949	58.95	25.4
Data set 3	11	5	16811	35446	53.75	51.95
Data set 4	19	8	20995	50616	28.9	25.65

Table 4. 1: Data sets input

Furthermore, it is imperative to document the specific threshold values and underlying assumptions employed during the implementation of the proposed framework the four data ses, and these parameters should be explicitly detailed in Table 4.2.

Variable / Threshold	Assumed value
d1	30.48 cm
d2	7.62 cm
User defined allowable reliability ratio	95 %
Common edge tolerance width	50 cm
Refinning initial space	200 cm
Minimum / Maximum wall width	30 / 60 cm
Minimum wall height	300 cm
Wall width step	5 cm
Wall height step	10 cm

Table 4. 2: The threshold values use in the proposed workflow.

4.2 Data set 1

The dataset comprises segmented point cloud data obtained from the indoor environment of the TUM, encompassing eight distinct rooms. Figure 4.5 visually represents the semantic floor and wall point cloud. Furthermore, the dataset covers information about the adjacency matrix, elucidating the spatial relationships among the various spaces.

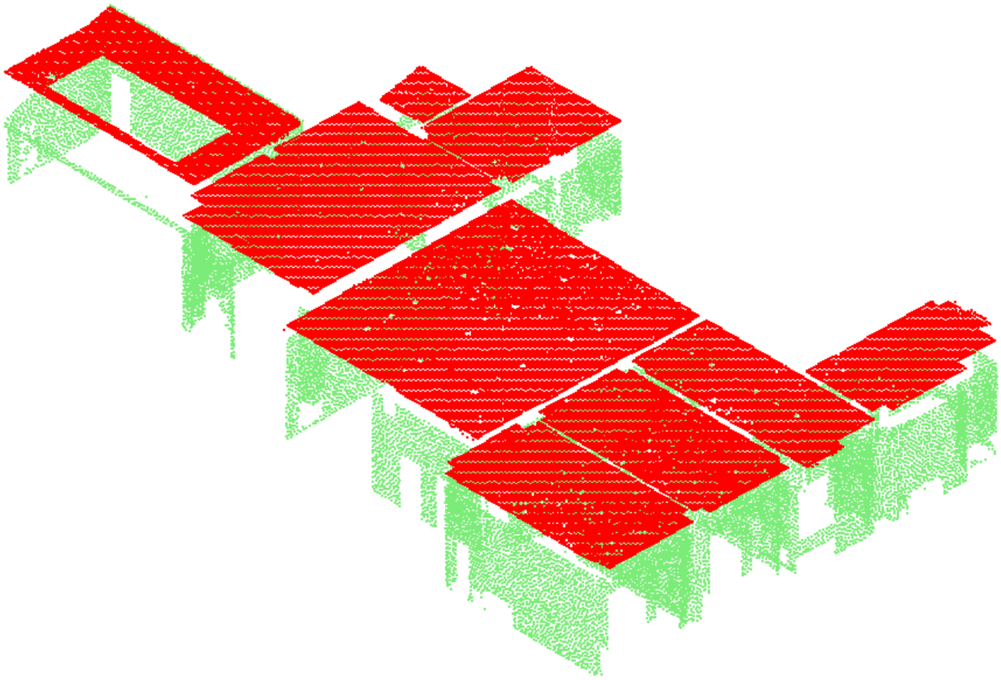

Figure 4. 1: The semantic segmented point cloud of Data set 1, walls (in green) and space-wise ceiling (in red)

Figure 4.6 presents the conclusive BIM model after the successful execution of the prescribed framework described in Chapter 3. This visualization exhibits the amalgamation of parameterized wall elements with segmented point clouds, thus illustrating the outcomes achieved through the framework's implementation.

The visual examination of the point cloud reveals a high level of quality and average density, as does the accuracy of the class segmentation performed on the point cloud. Some challenges are encountered in the segmentation of walls within room 1, suggesting the presence of concealed spaces within the same room.

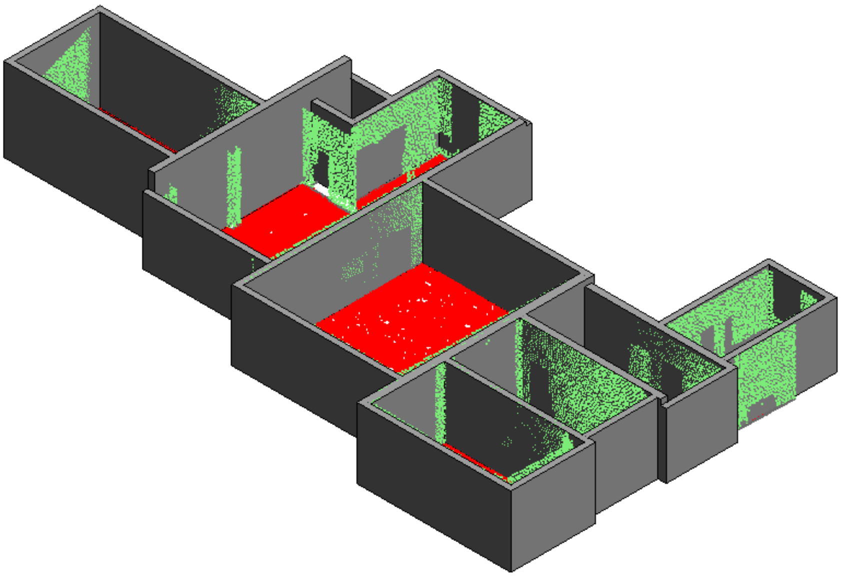

Figure 4. 2: The reconstructed BIM model of data set 1

However, the incidence of noise within the dataset is minimal. Furthermore, the computational execution time for the algorithm is about 13.8 seconds. In Figure 4.7, a top view of the generated rooms and walls are depicted, accompanied by their respective name tags.

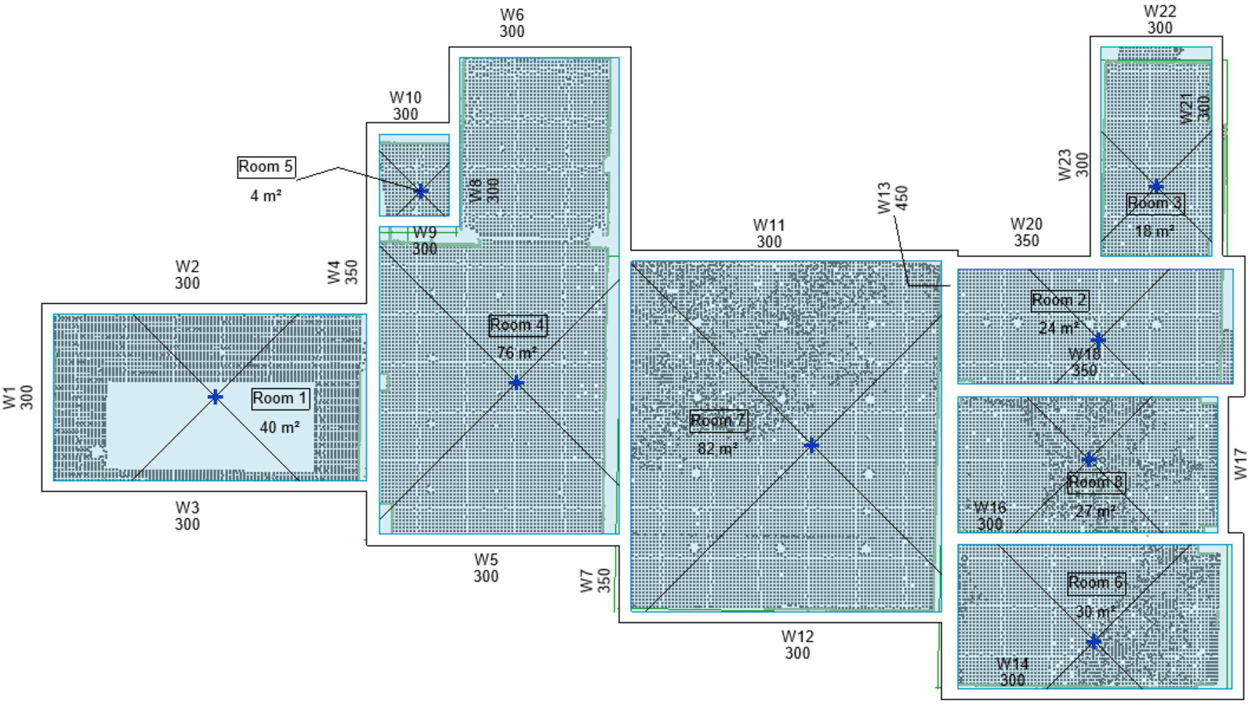

Figure 4. 3: Top view of rooms and walls of Data set 1

4.3 Data set 2

The dataset comprises segmented point cloud data obtained from the indoor environment of the TUM, encompassing 12 distinct rooms interconnected by a lengthy corridor. Figure 4.8 visually represents the semantic floor and wall point cloud. Furthermore, the dataset covers information about the adjacency matrix.

In Figure 4.9, a reconstructed BIM model of data set 2 is presented, illustrating the results of the applied framework after the execution. The run time is 22.4 sec.

Figure 4.10 depicts top views of the generated rooms and walls, accompanied by their respective name tags. The quality of the point cloud data in dataset 2 is generally commendable, except for instances of inadequate segmentation in the entrance and exit regions of the corridor. Notably, there are no discernible defects or errors within the dataset, except for minor room refinement discrepancies, which have been rectified through manual intervention.

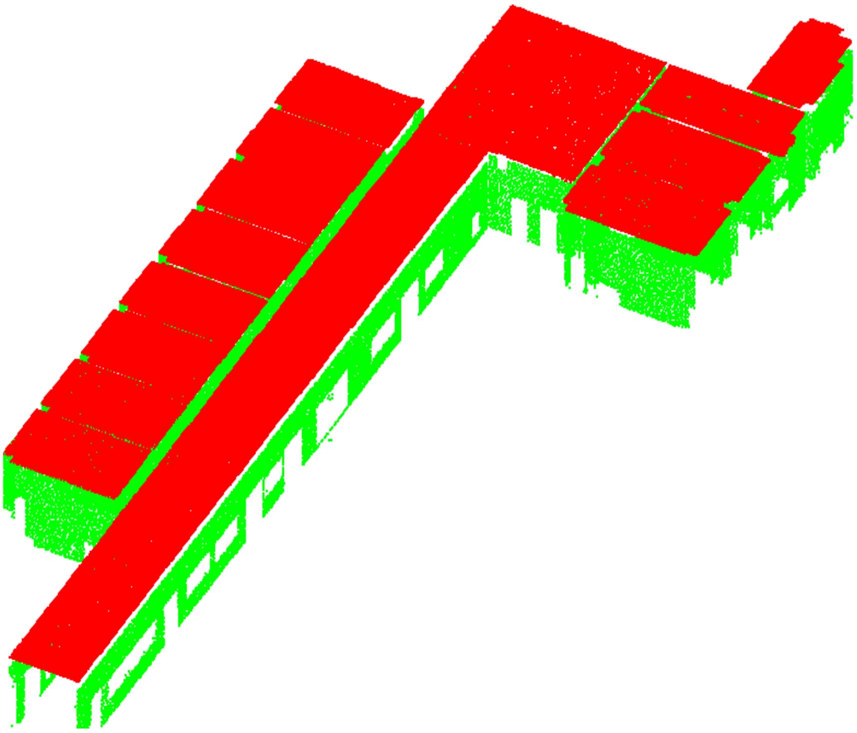

Figure 4. 4: The semantic segmented point cloud of Data set 2, walls (in green) and space-wise floor (in red)

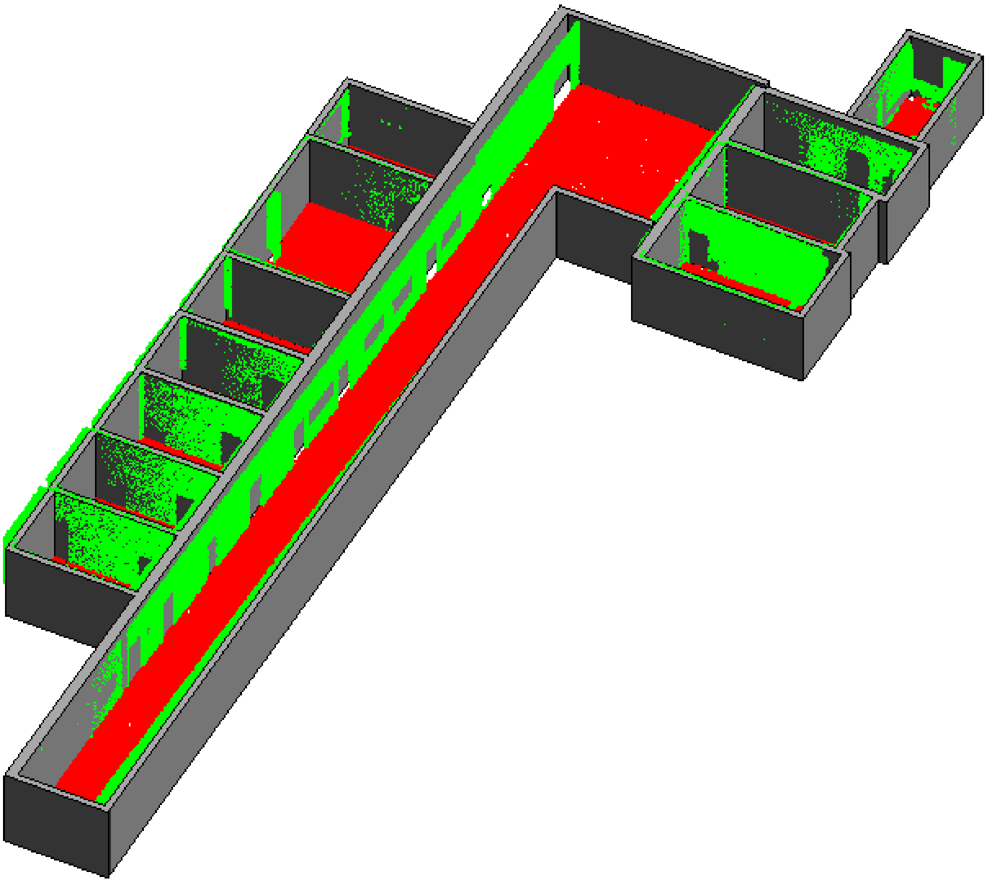

Figure 4. 5: The reconstructed BIM model of data set 2

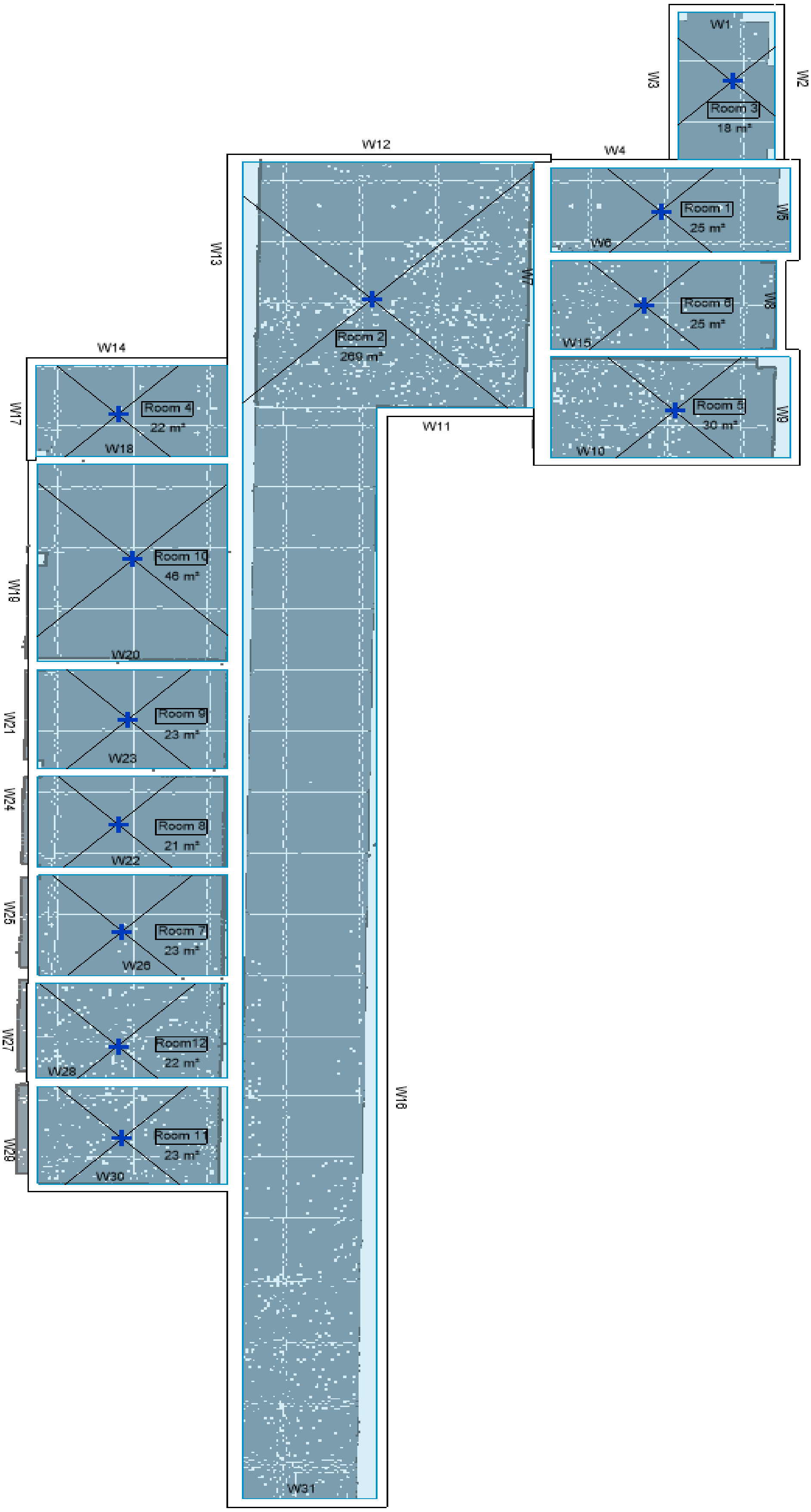

Figure 4. 6: A top view of rooms and walls of Data set 2

4.4 Data set 3

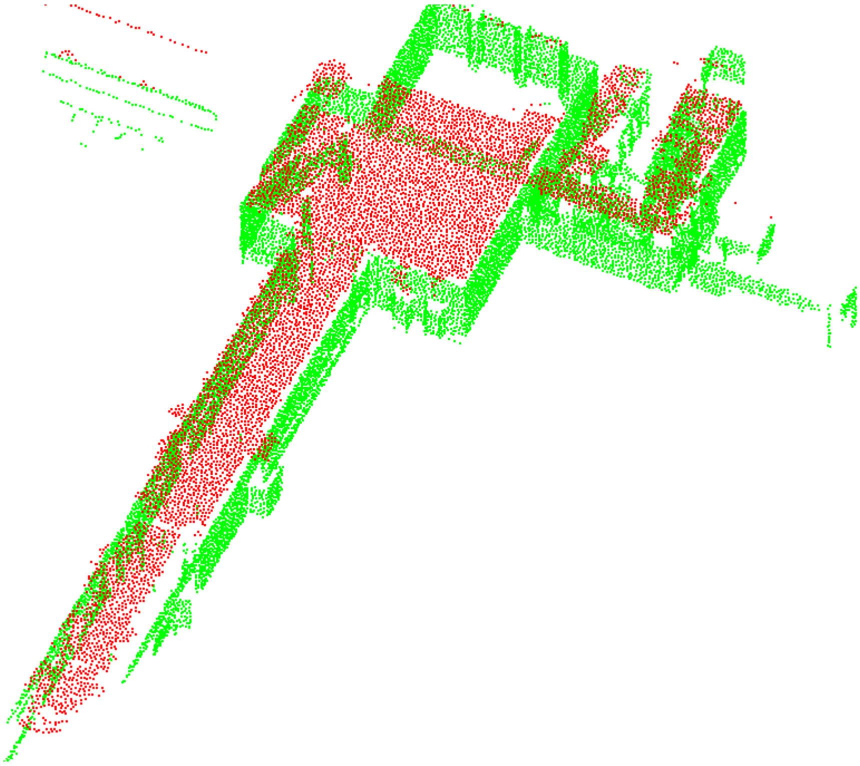

Figure 4. 7: The semantic segmented point cloud of Data set 3, walls (in green) and space-wise floor (in red)

Data Set 3 comprises a point cloud representation of 11 distinct rooms within a building located at Stanford University. Upon visual inspection, it is evident that this dataset exhibits several notable characteristics, which include discernible issues related to spatial boundaries and a substantial presence of noise artifacts, particularly within rooms numbered 1, 7, and 8. Moreover, there needs to be more data points within spaces 5 and 2, leading to compromised accuracy in delineating space boundaries. This decrease in data quality, coupled with the absence of well-defined space definitions as outlined in the algorithm detailed in Appendix A.1, further exacerbates the situation. Even after applying the algorithm for merging walls with overlapping regions within a range of 350 mm width, there are instances where walls remain unmerged, resulting in intersecting walls. The processing time for this dataset is approximately 10.4 seconds due to a remarkable decrease in the number of points in related point clouds compared to data sets 1 and 2.

Figure 4.11 presents semantic representations of wall and floor point clouds. Figure 4.12 showcases the reconstructed BIM model derived from the dataset. In Figure 4.13, a top view illustrates the wall and room tags superimposed on the point cloud.

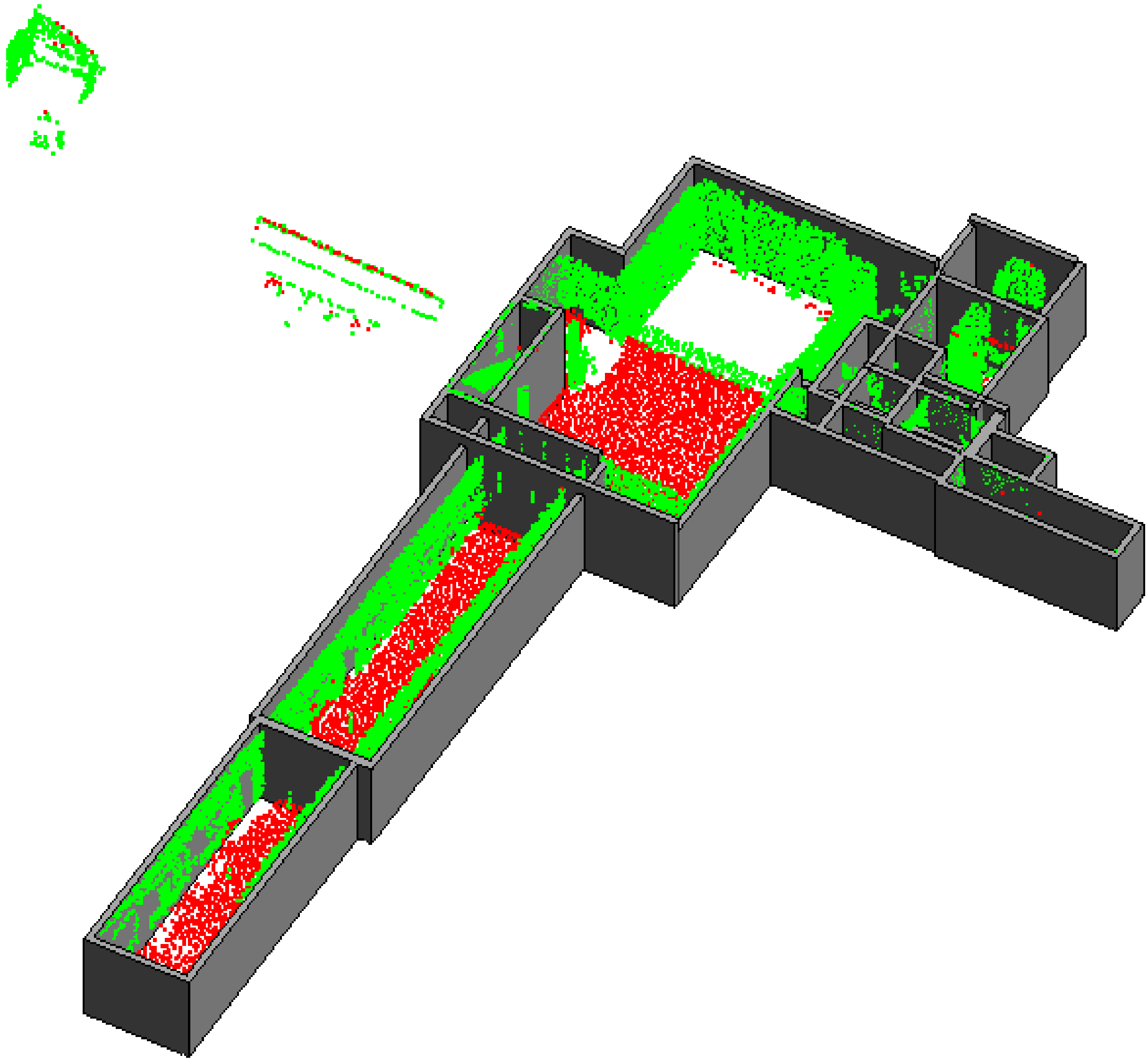

Figure 4. 8: The reconstructed BIM model of data set 3.

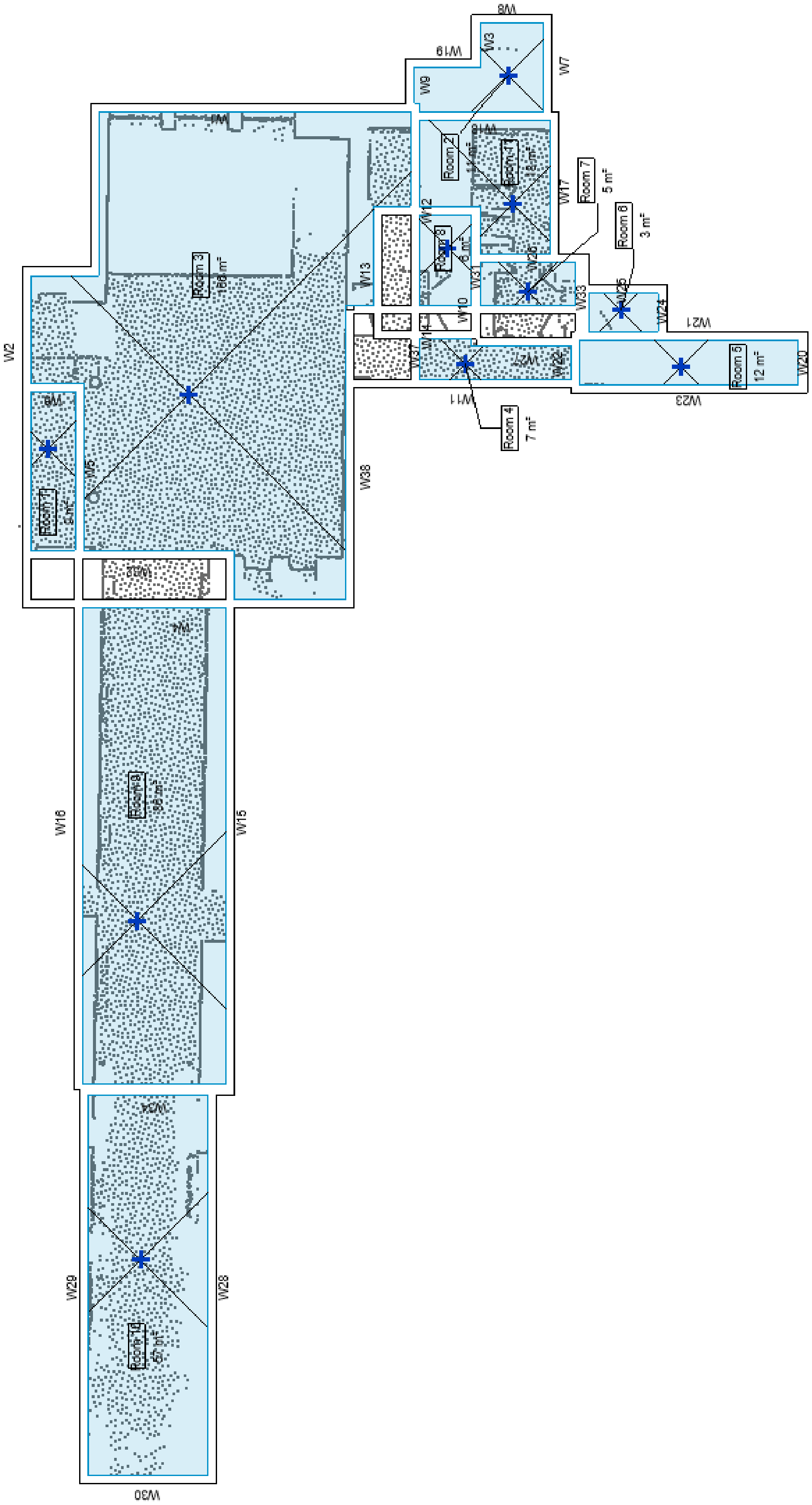

Figure 4. 9: Top view of labeled rooms and walls of Data set 3

4.5 Data set 4

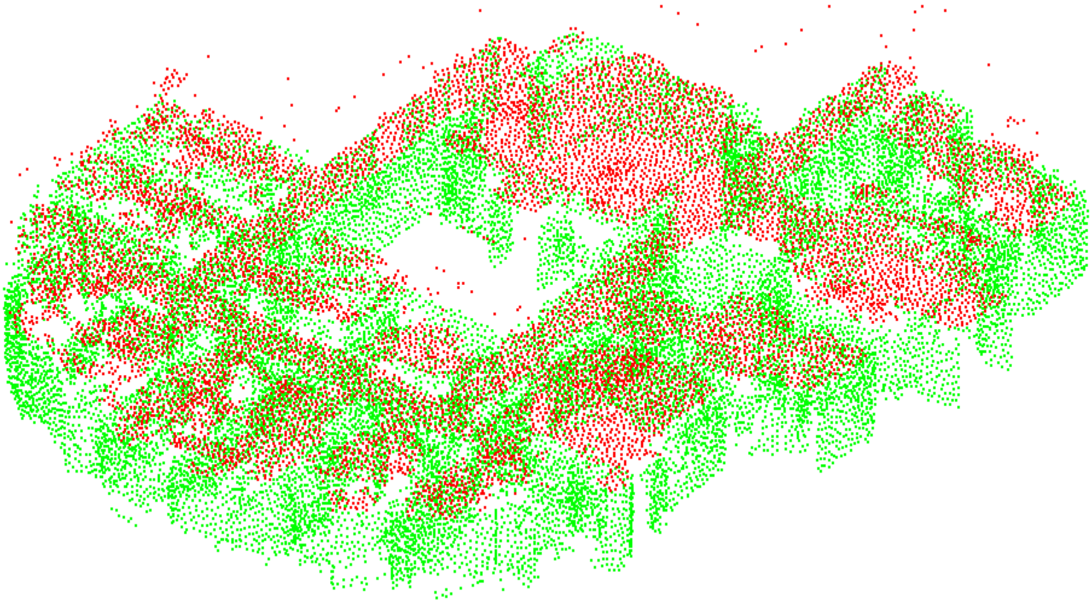

Figure 4. 10: The semantic segmented point cloud of Data set 4, walls (in green) and space-wise floor (in red)

Data Set 4 represents a complex dataset encompassing a point cloud derived from a building at Stanford University comprising 19 rooms that are spatially arranged based on the provided adjacency matrix. Figure 4.14 visually represents semantic floor and wall point clouds. Furthermore, the dataset encompasses information about the adjacency matrix.

Upon visual inspection, the quality of the point cloud appears to be satisfactory. Nonetheless, certain intricacies are discernible in the refinement of room boundaries. These intricacies manifest mainly in the merging of room boundaries, as exemplified by the amalgamation of rooms W49 and W47, which is depicted in Figure 4.16. Furthermore, there is a noticeable alteration in the minimum threshold for the determination of minimum wall heights, primarily because a substantial portion of the walls measure less than 3 meters in height. This alteration may be attributed to the presence of false ceilings within the building. Figure 4.15 depicts the constructed BIM models of Data set 4 of walls superimposed upon the segmented point cloud data. The processing time for this dataset is approximately 21.2 seconds.

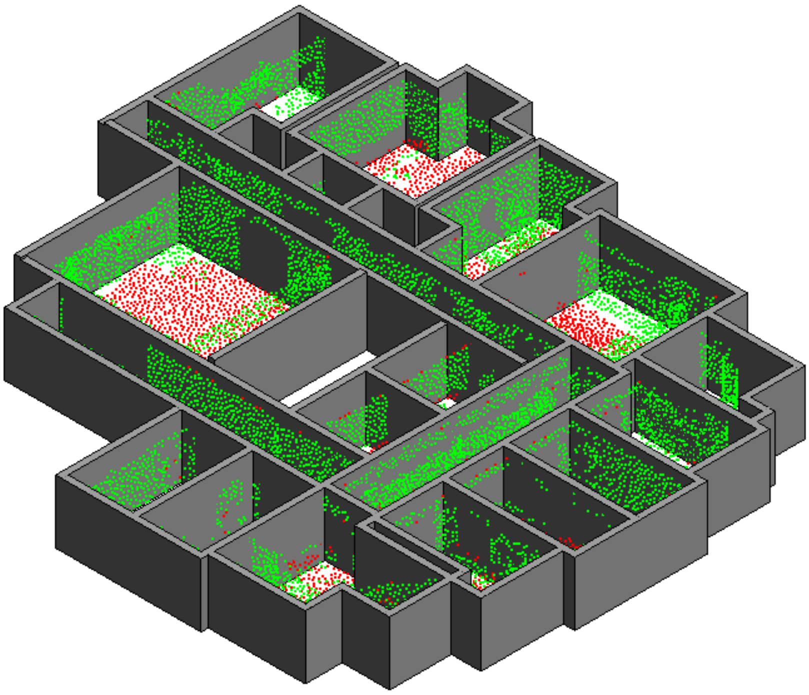

Figure 4. 11: The reconstructed BIM model of data set 4.

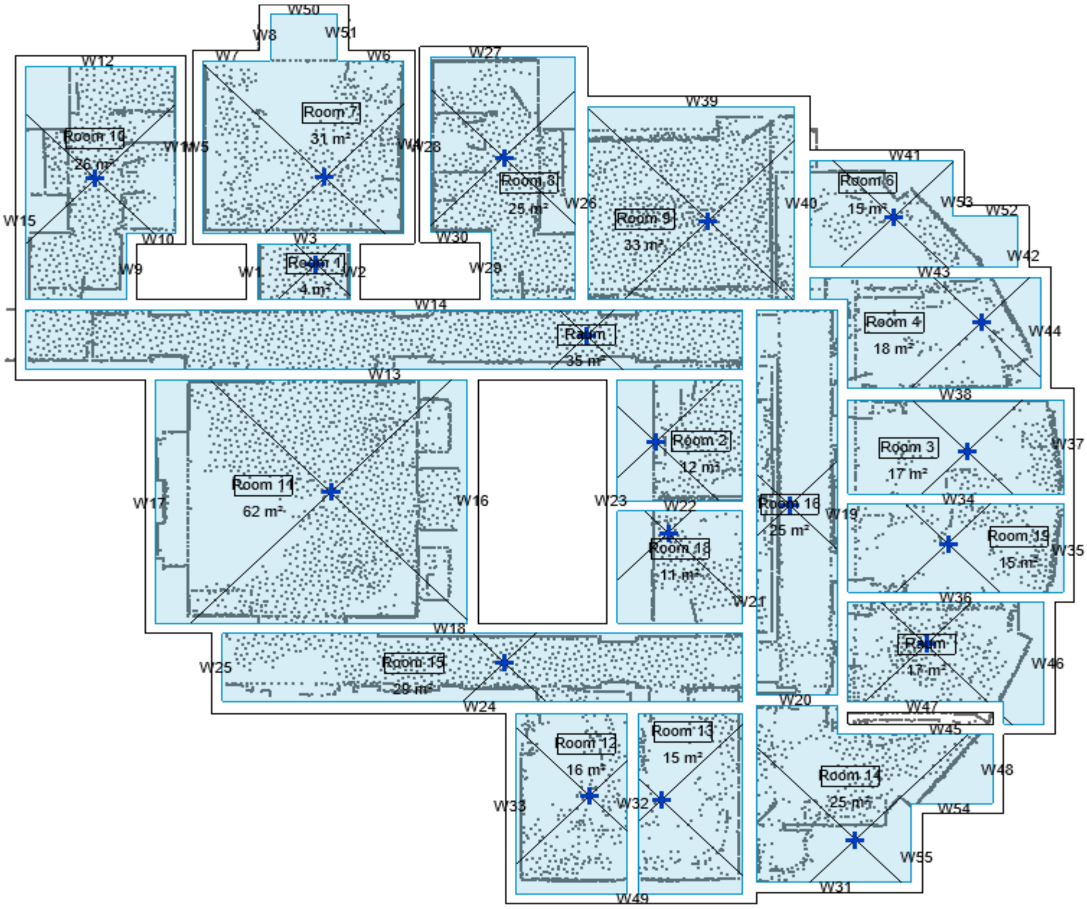

Figure 4. 12: Top view of labeled rooms and walls of Data set 4

4.6 Quantitative evaluation of model reconstruction

The reconstructed BIM model for each test dataset was subjected to a comparative analysis against the corresponding reference BIM model, focusing specifically on the wall dimension parameters (length, width, and height). Table 4.2 presents the average difference values across all walls within each dataset and reference BIM model. This tabulated data serves as a valuable resource for evaluating the accuracy of the reconstructed BIM model and provides insights into the degree of alignment achieved with respect to the reference BIM model.

Data sets	Parameters		
	δ Length (m)	δ Width (m)	δ Height (m)
Data set 1	0.08	0.05	0.08
Data set 2	0.15	0.09	0.06
Data set 3	0.12	0.06	0.05
Data set 4	0.17	0.11	0.07
Average	**0.13**	**0.08**	**0.07**

Table 4. 3: Quantitative evaluation of model construction

5 Conclusion and future work

5.1 Conclusion

Within this thesis, we have undertaken an exploration of the proposed framework designed for the conversion of indoor environment point cloud data into a parametrized BIM model. The resulting BIM model, as previously articulated, holds the potential to significantly impact diverse domains. The framework developed herein aims to address challenges encountered in prior research endeavors, particularly in relation to issues such as data volume.

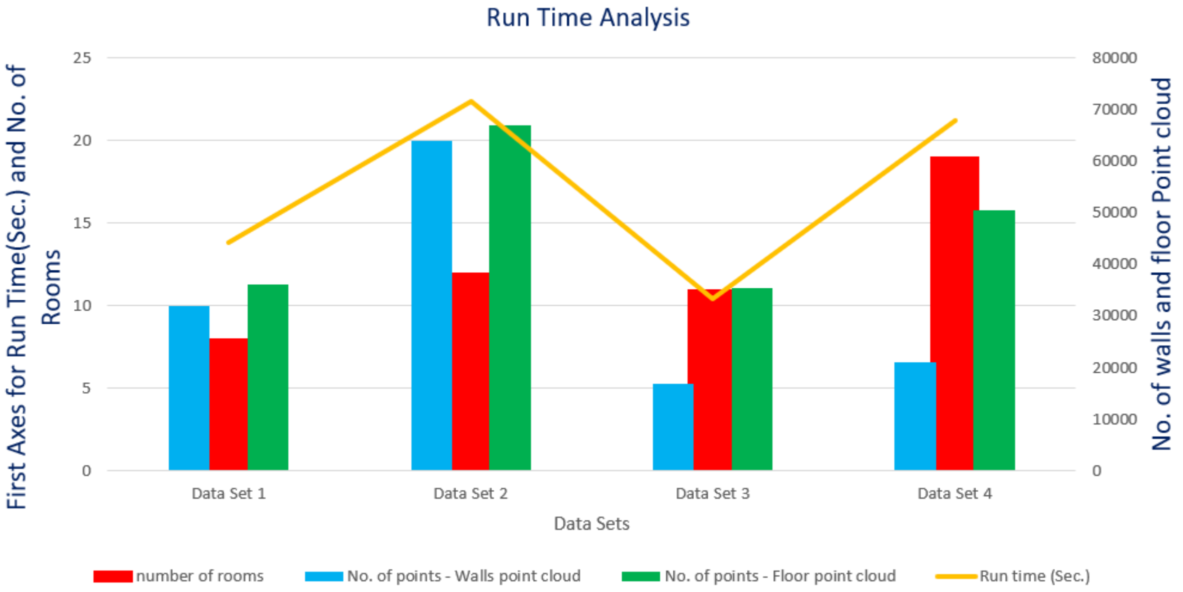

Figure 5. 1: Run time analysis of the 4 Data sets

Figure 5.1 presents the analysis results of the four datasets that have been previously discussed in Chapter 4 including the graph representations of the number of points within segmented floor spaces and wall point clouds, the number of rooms, and the associated run time for each.

It is evident from the analysis that the run time is closely correlated with the number of points. This relationship is primarily due to the utilization of multiple iterations within the algorithms embedded in the framework, as elucidated in the details provided in Appendix A. Furthermore, the modeling of wall elements in Revit and the number of rooms play crucial roles in determining the run time. It is important to note that the computational capabilities of the host computer may also influence the actual run time. Nevertheless, the analysis presented herein is intended for relative comparison among the different data sets.

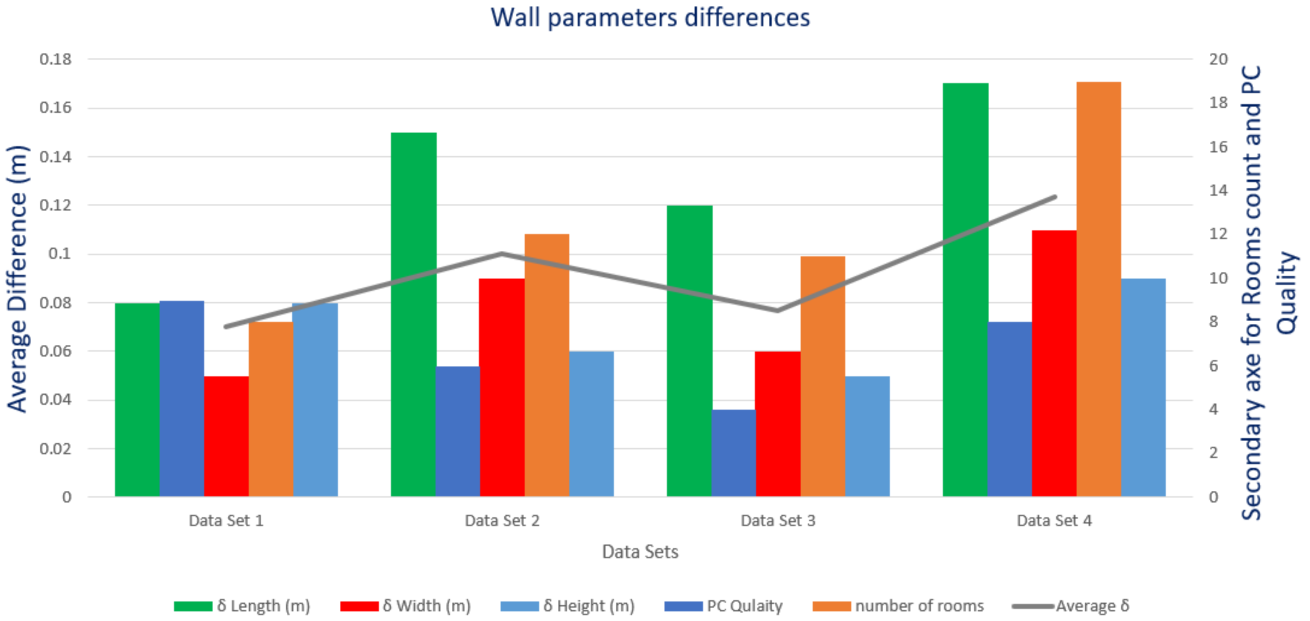

Figure 5. 2: Walls Parameter differences between the reconstructed and the reference BIM models

Figure 5.2 presents a comprehensive analysis of the four data sets. It involves the graphical representation of the data sets and their correlation with the average difference in wall dimensions between the created parameterized BIM model and the point cloud data. Those readings are depicted in the primary axes. In addition, the number of rooms and the quality of the point cloud within each data set are visually observed on the secondary axes.

Notably, the results indicate that the precision of the BIM model is affected by the quality of the point cloud. However, an increase in the number of rooms or a rise in the complexity of room boundaries within the point cloud data is associated with a decrease in the accuracy of the generated BIM model. There are multiple avenues for potential enhancements within the present framework. These considerations encompass the need for a meticulous assessment of the quality of segmented point clouds, particularly in relation to their spatial distribution. This scrutiny serves as a vital precautionary measure to mitigate potential challenges, a significance underscored by the complexities encountered in Data set 3.

Eventually, the workflow proposed in the thesis was adopted. Enabling the creation of a parametric BIM derived from semantic space-wise point cloud data and adjacency matrices can be employed. The resultant model outputs demonstrate a level of accuracy that can competitively compare with outcomes obtained through alternative frameworks suffering from data sizing. However, the pivotal determinant of accuracy rests in the quality of the initial point cloud data. Moreover, it is essential to acknowledge that this framework may not represent the optimal solution for processing large-scale point clouds. In such cases, further research and adaptations may be necessary to address the unique challenges posed by extensive and complex datasets.

5.2 Limitations and future works

The proposed framework exhibits certain limitations, which can be delineated as follows:

- In the realm of room refinement, a novel approach to partitioning rooms into rectangles, as expounded upon in section 3.4.2, is introduced. The proposal advocates the implementation of a convex hull algorithm, elucidated in Appendices B.1 and B.2, as a promising solution to rectify issues arising from non-rectangular, irregular room geometries. It is noteworthy that this adjustment may impact computational time, given the necessity for multiple passes through the spatial point data.
- It is logically expected that the walls of a room exhibit consistent or uniform height. Nevertheless, it is noteworthy that the presented framework does not address this constraint, as evidenced in Figure 5.3. Therefore, it is advisable to consider the incorporation of these limitations in subsequent developmental efforts. This change in procedure is designed to improve the consistency and accuracy of defining room boundaries.

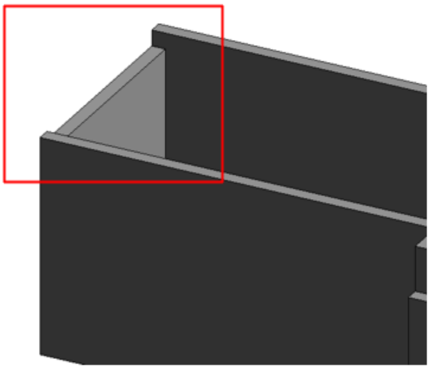

Figure 5. 3: Difference in wall heights of the same room

- The current wall thickness determination method needs to be more investigated. As detailed in section 3.4.3, the existing algorithm employs the assignment of the semantic wall point cloud to the assigned wall through grouping them by checking each point existence inside the wall's bounding box. However, assigning might be better grouping them by assigning each point to the nearest wall as shown in figure 5.4.

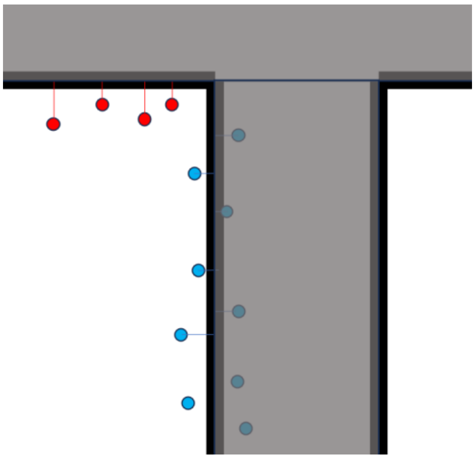

Figure 5. 4: Alternative procedure for points assignment to the corresponding walls

- Development for refinement and automation of the process involves developing a mechanism to identify wall openings, such as windows or doors, from the segmented wall point cloud and to be modeled in the reconstructed BIM model.
- A significant suggestion pertains to adopting a global parameterization approach akin to Autodesk Revit for defining wall coordinates. This transition promises increased flexibility in wall positioning, allowing for effortless modifications through the implementation of optimizing architectural design layout algorithms for creating functional and efficient spaces. Those algorithms should respect two fundamental aspects: space usage optimization and accessibility optimization. Space usage optimization focuses on maximizing space utility while minimizing wastage, achieved through strategic placement of structures, furniture, and amenities. This not only reduces the environmental footprint but also promotes sustainable resource utilization. Accessibility optimization aims to create spaces inclusive of individuals with diverse needs, aligning with universal design principles to enhance inclusivity.

References

Abreu, N., Pinto, A., Matos, A., & Pires, M. (2023). Procedural Point Cloud Modelling in Scan-to-BIM and Scan-vs-BIM Applications: A Review. *ISPRS International Journal of Geo-Information*, *12*(7), 260. https://doi.org/10.3390/ijgi12070260

Abu-Hamd, M. (2015). Implementation of BIM into cold-formed steel residential buildings. *Building Information Modelling (BIM) in Design, Construction and Operations*, *1*(September 2015), 449–460. https://doi.org/10.2495/bim150371

Adan, A., & Huber, D. (2011). 3D reconstruction of interior wall surfaces under occlusion and clutter. *Proceedings - 2011 International Conference on 3D Imaging, Modeling, Processing, Visualization and Transmission, 3DIMPVT 2011*, 275–281. https://doi.org/10.1109/3DIMPVT.2011.42

Adán, A., Ramón, A., Vivancos, J. L., Vilar, A., & Aparicio-Fernández, C. (2023). Automatic generation of as-is BEM models of buildings. *Journal of Building Engineering*, *73*(May), 106865. https://doi.org/10.1016/j.jobe.2023.106865

Akanmu, A. A., Anumba, C. J., & Ogunseiju, O. O. (2021). Towards next generation cyber-physical systems and digital twins for construction. *Journal of Information Technology in Construction*, *26*(July), 505–525. https://doi.org/10.36680/j.itcon.2021.027

Alizadehsalehi, S., & Yitmen, I. (2023). Digital twin-based progress monitoring management model through reality capture to extended reality technologies (DRX). *Smart and Sustainable Built Environment*, *12*(1), 200–236. https://doi.org/10.1108/SASBE-01-2021-0016

Andriasyan, M., Moyano, J., Nieto-Julián, J. E., & Antón, D. (2020). From point cloud data to Building Information Modelling: An automatic parametric workflow for heritage. *Remote Sensing*, *12*(7). https://doi.org/10.3390/rs12071094

Armeni, I., Sener, O., Zamir, A. R., Jiang, H., Brilakis, I., Fischer, M., & Savarese, S. (2016). *3D Semantic Parsing of Large-Scale Indoor Spaces (a) Raw Point Cloud (b) Space Parsing and Alignment in Canonical 3D Space (c) Building Element Detection*. 1534–1543. https://doi.org/10.1109/CVPR.2016.170

Azhar, S. (2011). Building information modeling (BIM): Trends, benefits, risks, and challenges for the AEC industry. *Leadership and Management in Engineering*, *11*(3), 241–252. https://doi.org/10.1061/(ASCE)LM.1943-5630.0000127

Barazzetti, L. (2016). Parametric as-built model generation of complex shapes from point clouds. *Advanced Engineering Informatics*, *30*(3), 298–311. https://doi.org/10.1016/j.aei.2016.03.005

Becerik-Gerber, B., Jazizadeh, F., Li, N., & Calis, G. (2012). Application Areas and Data Requirements for BIM-Enabled Facilities Management. *Journal of Construction Engineering and Management*, *138*(3), 431–442. https://doi.org/10.1061/(asce)co.1943-7862.0000433

Bello, S. A., Yu, S., Wang, C., Adam, J. M., & Li, J. (2020). Review: Deep learning on 3D point clouds. *Remote Sensing*, *12*(11). https://doi.org/10.3390/rs12111729

Besl, P. J., & McKay, N. D. (1992). A Method for Registration of 3-D Shapes. In *IEEE Transactions on Pattern Analysis and Machine Intelligence* (Vol. 14, Issue 2, pp. 239–256). https://doi.org/10.1109/34.121791

Betsas, T., & Georgopoulos, A. (2022). Point-Cloud Segmentation for 3D Edge Detection and Vectorization. *Heritage*, *5*(4), 4037–4060. https://doi.org/10.3390/heritage5040208

Boje, C., Guerriero, A., Kubicki, S., & Rezgui, Y. (2020). Towards a semantic Construction Digital Twin: Directions for future research. *Automation in Construction*, *114*(January), 103179. https://doi.org/10.1016/j.autcon.2020.103179

Bolton A. (2018). Gemini Principles. *CDBB*. https://doi.org/10.17863/CAM.32260

Borrmann, A., König, M., Koch, C., & Beetz, J. (2018). Building information modeling: Technology foundations and industry practice. *Building Information Modeling: Technology Foundations and Industry Practice*, 1–584. https://doi.org/10.1007/978-3-319-92862-3

Bortoluzzi, B., Efremov, I., Medina, C., Sobieraj, D., & McArthur, J. J. (2019). Automating the creation of building information models for existing buildings. *Automation in Construction*, *105*(March), 102838. https://doi.org/10.1016/j.autcon.2019.102838

Bosché, F., Ahmed, M., Turkan, Y., Haas, C. T., & Haas, R. (2015). The value of integrating Scan-to-BIM and Scan-vs-BIM techniques for construction monitoring using laser scanning and BIM: The case of cylindrical MEP components. *Automation in Construction*, *49*, 201–213. https://doi.org/10.1016/j.autcon.2014.05.014

Budroni, A., & Boehm, J. (2010). Automated 3D Reconstruction of Interiors from Point Clouds. *International Journal of Architectural Computing*, *8*(1), 55–73. https://doi.org/10.1260/1478-0771.8.1.55

Buldo, M., Agustin-Hernandez, L., Verdoscia, C., & Tavolare, R. (2023). A scan-To-bim workflow proposal for cultural heritage. automatic point cloud segmentation and parametric-Adaptive modelling of vaulted systems. *International Archives of the Photogrammetry, Remote Sensing and Spatial Information Sciences - ISPRS Archives*, *48*(M-2–2023), 333–340. https://doi.org/10.5194/isprs-Archives-XLVIII-M-2-2023-333-2023

Burgmann, R., Rosen, P. A., & Fielding, E. J. (2000). Synthetic aperture radar interferometry to measure earth’s surface topography and its deformation. *Annual Review of Earth and Planetary Sciences*, *28*(January 2015), 169–209. https://doi.org/10.1146/annurev.earth.28.1.169

Charef, R., Alaka, H., & Emmitt, S. (2018). Beyond the third dimension of BIM: A systematic review of literature and assessment of professional views. *Journal of Building Engineering*, *19*, 242–257. https://doi.org/10.1016/j.jobe.2018.04.028

Che, E., Jung, J., & Olsen, M. J. (2019). Object recognition, segmentation, and classification of mobile laser scanning point clouds: A state of the art review. *Sensors (Switzerland)*, *19*(4). https://doi.org/10.3390/s19040810

Chen, C., Yang, B., Song, S., Tian, M., Li, J., Dai, W., & Fang, L. (2018). Calibrate multiple consumer RGB-D cameras for low-cost and efficient 3D indoor mapping. *Remote Sensing*, *10*(2), 1–29. https://doi.org/10.3390/rs10020328

Collings, D. G., Scullion, H., & Vaiman, V. (2015). Talent management: Progress and prospects. *Human Resource Management Review*, *25*(3), 233–235. https://doi.org/10.1016/j.hrmr.2015.04.005

Cui, Y., Chen, R., Chu, W., Chen, L., Tian, D., Li, Y., & Cao, D. (2022). Deep Learning for Image and Point Cloud Fusion in Autonomous Driving: A Review. *IEEE Transactions on Intelligent Transportation Systems*, *23*(2), 722–739. https://doi.org/10.1109/TITS.2020.3023541

Davila Delgado, J. M., & Oyedele, L. (2021). Digital Twins for the built environment: learning from conceptual and process models in manufacturing. *Advanced Engineering Informatics*, *49*(May), 101332. https://doi.org/10.1016/j.aei.2021.101332

Donato, V. (2015). *Transformability of the Existing Buildings: an approach based on BIM technologies*. *November 2014*, 212.

Eastman, C., Liston, K., Sacks, R., & Liston, K. (2008). *BIM Handbook Paul Teicholz Rafael Sacks*.

Elhashash, M., Albanwan, H., & Qin, R. (2022). A Review of Mobile Mapping Systems: From Sensors to Applications. *Sensors*, *22*(11), 1–26. https://doi.org/10.3390/s22114262

Elmualim, A., Shockley, D., Valle, R., Ludlow, G., & Shah, S. (2010). Barriers and commitment of facilities management profession to the sustainability agenda. *Building and Environment*, *45*(1), 58–64. https://doi.org/10.1016/j.buildenv.2009.05.002

Engelmann, F., Kontogianni, T., Hermans, A., & Leibe, B. (2017). Exploring Spatial Context for 3D Semantic Segmentation of Point Clouds. *Proceedings - 2017 IEEE International Conference on Computer Vision Workshops, ICCVW 2017*, *2018-Janua*, 716–724. https://doi.org/10.1109/ICCVW.2017.90

Gholizadeh, P., Behzad, E., & Memarian, B. (2018). Construction Research Congress 2018 725. *Construction Research Congress 2018 Downloaded*, *2010*(2012), 725–735.

Gurevich, U., & Sacks, R. (2020). Longitudinal Study of BIM Adoption by Public Construction Clients. *Journal of Management in Engineering*, *36*(4). https://doi.org/10.1061/(asce)me.1943-5479.0000797

Hackel, T., Savinov, N., Ladicky, L., Wegner, J. D., Schindler, K., & Pollefeys, M. (2017). Semantic3D.Net: a New Large-Scale Point Cloud Classification Benchmark. *ISPRS Annals of the Photogrammetry, Remote Sensing and Spatial*

Information Sciences, *4*(1W1), 91–98. https://doi.org/10.5194/isprs-annals-IV-1-W1-91-2017

He, Y., Yu, H., Liu, X., Yang, Z., Sun, W., Wang, Y., Fu, Q., Zou, Y., & Mian, A. (2021). *Deep Learning based 3D Segmentation: A Survey*. http://arxiv.org/abs/2103.05423

Heo, J., Jeong, S., Park, H. K., Jung, J., Han, S., Hong, S., & Sohn, H. G. (2013). Productive high-complexity 3D city modeling with point clouds collected from terrestrial LiDAR. *Computers, Environment and Urban Systems*, *41*, 26–38. https://doi.org/10.1016/j.compenvurbsys.2013.04.002

Hosamo, H. H., Nielsen, H. K., Kraniotis, D., Svennevig, P. R., & Svidt, K. (2023). Improving building occupant comfort through a digital twin approach: A Bayesian network model and predictive maintenance method. *Energy and Buildings*, *288*, 112992. https://doi.org/10.1016/j.enbuild.2023.112992

Hu, Q., Yang, B., Xie, L., Rosa, S., Guo, Y., Wang, Z., Trigoni, N., & Markham, A. (2022). Learning Semantic Segmentation of Large-Scale Point Clouds With Random Sampling. *IEEE Transactions on Pattern Analysis and Machine Intelligence*, *44*(11), 8338–8354. https://doi.org/10.1109/TPAMI.2021.3083288

Javadnejad, F., Gillins, D. T., Parrish, C. E., & Slocum, R. K. (2020). A photogrammetric approach to fusing natural colour and thermal infrared UAS imagery in 3D point cloud generation. *International Journal of Remote Sensing*, *41*(1), 211–237. https://doi.org/10.1080/01431161.2019.1641241

Kaewunruen, S., & Lian, Q. (2019). Digital twin aided sustainability-based lifecycle management for railway turnout systems. *Journal of Cleaner Production*, *228*, 1537–1551. https://doi.org/10.1016/j.jclepro.2019.04.156

Kantaros, A., Ganetsos, T., & Petrescu, F. I. T. (2023). Three-Dimensional Printing and 3D Scanning: Emerging Technologies Exhibiting High Potential in the Field of Cultural Heritage. *Applied Sciences (Switzerland)*, *13*(8). https://doi.org/10.3390/app13084777

Koide, K., Oishi, S., Yokozuka, M., & Banno, A. (2023). *Exact Point Cloud Downsampling for Fast and Accurate Global Trajectory Optimization*. http://arxiv.org/abs/2307.02948

Kor, M., Yitmen, I., & Alizadehsalehi, S. (2023). An investigation for integration of deep learning and digital twins towards Construction 4.0. *Smart and Sustainable Built Environment*, *12*(3), 461–487. https://doi.org/10.1108/SASBE-08-2021-0148

Landrieu, L., & Boussaha, M. (2019). Point cloud oversegmentation with graph-structured deep metric learning. *Proceedings of the IEEE Computer Society Conference on Computer Vision and Pattern Recognition*, *2019-June*, 7432–7441. https://doi.org/10.1109/CVPR.2019.00762

Li, W., Mo, W., Zhang, X., Squiers, J. J., Lu, Y., Sellke, E. W., Fan, W., DiMaio, J. M., & Thatcher, J. E. (2015). Outlier detection and removal improves accuracy of machine learning approach to multispectral burn diagnostic imaging. *Journal of Biomedical Optics*, *20*(12), 121305. https://doi.org/10.1117/1.jbo.20.12.121305

Lu, R., & Brilakis, I. (2019). Digital twinning of existing reinforced concrete bridges from labelled point clusters. *Automation in Construction*, *105*(May), 102837. https://doi.org/10.1016/j.autcon.2019.102837

Macher, H., Landes, T., & Grussenmeyer, P. (2017). From point clouds to building information models: 3D semi-automatic reconstruction of indoors of existing buildings. *Applied Sciences (Switzerland)*, *7*(10), 1–30. https://doi.org/10.3390/app7101030

Max Rodriguez. (2022). *BIM Dimensions*. What Are BIM Dimensions? (4D, 5D, 6D,7D). https://www.structuresinsider.com/post/dimensions-of-bim-explained

Mehranfar, M., Braun, A., & Borrmann, A. (2022). *Automatic creation of digital building twins with rich semantics from dense RGB point clouds through semantic segmentation and model fitting*. 1–10.

Meng, H. Y., Gao, L., Lai, Y. K., & Manocha, Di. (2019). VV-net: Voxel VAE net with group convolutions for point cloud segmentation. *Proceedings of the IEEE International Conference on Computer Vision*, *2019-October*(July 2021), 8499–8507. https://doi.org/10.1109/ICCV.2019.00859

Michael Grieves and John Vickers. (2017). Digital Twin: Mitigating Unpredictable, Undesirable Emergent Behavior in Complex Systems. In *Digital Twin: Mitigating Unpredictable, Undesirable Emergent Behavior in Complex Systems* (Issue Aug 2017). https://doi.org/10.1007/978-3-319-38756-7

Mielcarek, M., Kamińska, A., & Stereńczak, K. (2020). Digital aerial photogrammetry (DAP) and airborne laser scanning (ALS) as sources of information about tree height: Comparisons of the accuracy of remote sensing methods for tree height estimation. *Remote Sensing*, *12*(11). https://doi.org/10.3390/rs12111808

Monszpart, A., Mellado, N., Brostow, G. J., & Mitra, N. J. (2015). RAPter: Rebuilding man-made scenes with regular arrangements of planes. *ACM Transactions on Graphics*, *34*(4). https://doi.org/10.1145/2766995

Montgomery, J., Wartman, J., Reed, A. N., Gallant, A. P., Hutabarat, D., & Mason, H. B. (2021). Field reconnaissance data from GEER investigation of the 2018 MW 7.5 Palu-Donggala earthquake. *Data in Brief*, *34*, 106742. https://doi.org/10.1016/j.dib.2021.106742

Mora, T. D., Bolzonello, E., Cavalliere, C., & Peron, F. (2020). Key parameters featuring bim-lca integration in buildings: A practical review of the current trends. *Sustainability (Switzerland)*, *12*(17), 1–33. https://doi.org/10.3390/su12177182

Moretti, N., Ellul, C., Re Cecconi, F., Papapesios, N., & Dejaco, M. C. (2021). GeoBIM for built environment condition assessment supporting asset management decision making. *Automation in Construction*, *130*(November 2020), 103859. https://doi.org/10.1016/j.autcon.2021.103859

Mura, C., Mattausch, O., & Pajarola, R. (2016). Piecewise-planar Reconstruction of Multi-room Interiors with Arbitrary Wall Arrangements. *Computer Graphics Forum*, *35*(7), 179–188. https://doi.org/10.1111/cgf.13015

Nguyen, T. D., & Adhikari, S. (2023). The Role of BIM in Integrating Digital Twin in Building Construction: A Literature Review. *Sustainability (Switzerland)*, *15*(13), 1–26. https://doi.org/10.3390/su151310462

Niemeyer, J., Rottensteiner, F., & Soergel, U. (2014). Contextual classification of lidar data and building object detection in urban areas. *ISPRS Journal of Photogrammetry and Remote Sensing*, *87*, 152–165. https://doi.org/10.1016/j.isprsjprs.2013.11.001

Nikoohemat, S., Peter, M., Oude Elberink, S., & Vosselman, G. (2017). EXPLOITING INDOOR MOBILE LASER SCANNER TRAJECTORIES for SEMANTIC INTERPRETATION of POINT CLOUDS. *ISPRS Annals of the Photogrammetry,* *Remote Sensing and Spatial Information Sciences*, *4*(2W4), 355–362. https://doi.org/10.5194/isprs-annals-IV-2-W4-355-2017

Ochmann, S., Vock, R., & Klein, R. (2019). Automatic reconstruction of fully volumetric 3D building models from oriented point clouds. *ISPRS Journal of Photogrammetry and Remote Sensing*, *151*(March), 251–262. https://doi.org/10.1016/j.isprsjprs.2019.03.017

Ochmann, S., Vock, R., Wessel, R., & Klein, R. (2016). Automatic reconstruction of parametric building models from indoor point clouds. *Computers and Graphics (Pergamon)*, *54*(July), 94–103. https://doi.org/10.1016/j.cag.2015.07.008

Okorn, B., Xiong, X., Akinci, B., & Huber, D. (2010). Toward Automated Modeling of Floor Plans. *Proceedings of the Symposium on 3D Data Processing, Visualization and Transmission*, *2*. http://swing.adm.ri.cmu.edu/pub_files/2010/5/2009 3DPVT plan view modeling v13 (resubmitted).pdf

Oliver Eischet. (2023). *Level of Development (LOD): Looking at BIM Data across the Building Lifecycle.* Medium. https://medium.com/specter-automation-insights/level-of-development-lod-looking-at-bim-data-across-the-building-lifecycle-7477fee5cc83

Pepe, M., Costantino, D., Alfio, V. S., Restuccia, A. G., & Papalino, N. M. (2021). Scan to BIM for the digital management and representation in 3D GIS environment of cultural heritage site. *Journal of Cultural Heritage*, *50*, 115–125. https://doi.org/10.1016/j.culher.2021.05.006

Rabbani, T., van den Heuvel, F. A., & Vosselman, G. (2006). Segmentation of Point Clouds using Smoothness Constraints. *{I}nternational{A}rchives of the {P}hotogrammetry, {R}emote {S}ensing and {S}patial {I}nformation {S}ciences*, *36*(5), 248–253.

Rakotosaona, M. J., La Barbera, V., Guerrero, P., Mitra, N. J., & Ovsjanikov, M. (2020). PointCleanNet: Learning to Denoise and Remove Outliers from Dense Point Clouds. *Computer Graphics Forum*, *39*(1), 185–203. https://doi.org/10.1111/cgf.13753

Ren, X., Bo, L., & Fox, D. (2012). *RGB- (D) Scene Labeling : Features and Algorithms*. *D*, 2759–2766.

Sacks, R., Brilakis, I., Pikas, E., Xie, H. S., & Girolami, M. (2020). Construction with digital twin information systems. *Data-Centric Engineering*, *1*(6). https://doi.org/10.1017/dce.2020.16

Sampath, A., & Shan, J. (2010). Segmentation and reconstruction of polyhedral building roofs from aerial lidar point clouds. *IEEE Transactions on Geoscience and Remote Sensing*, *48*(3 PART2), 1554–1567. https://doi.org/10.1109/TGRS.2009.2030180

Schleich, B., Anwer, N., Mathieu, L., & Wartzack, S. (2017). Shaping the digital twin for design and production engineering. *CIRP Annals - Manufacturing Technology*, *66*(1), 141–144. https://doi.org/10.1016/j.cirp.2017.04.040

Sepasgozar, S. M. E., Khan, A. A., Smith, K., Romero, J. G., Shen, X., Shirowzhan, S., Li, H., & Tahmasebinia, F. (2023). BIM and Digital Twin for Developing Convergence Technologies as Future of Digital Construction. *Buildings*, *13*(2). https://doi.org/10.3390/buildings13020441

Siemers, F. M., & Bajorath, J. (2023). Differences in learning characteristics between support vector machine and random forest models for compound classification revealed by Shapley value analysis. *Scientific Reports*, *13*(1), 1–12. https://doi.org/10.1038/s41598-023-33215-x

Silberman, N., Hoiem, D., Kohli, P., & Fergus, R. (2012). Indoor segmentation and support inference from RGBD images Lecture Notes in Computer Science. *ECCV'12: Proceedings of the 12th European Conference on Computer Vision - Volume Part V*, *Part V*(Chapter 54), 746–760. http://www.springerlink.com/index/pdf/10.1007/978-3-642-33715-4_54%0Ahttp://link.springer.com/10.1007/978-3-642-33715-4_54%0Ahttp://dl.acm.org/citation.cfm?id=2403195

Tang, L., Chen, C., Tang, S., Wu, Z., & Trofimova, P. (2017). Building Information Modeling and Building Performance Optimization. In *Encyclopedia of Sustainable Technologies* (Vol. 2). Elsevier. https://doi.org/10.1016/B978-0-12-409548-9.10200-3

Tang, P., Huber, D., Akinci, B., Lipman, R., & Lytle, A. (2010). Automatic reconstruction of as-built building information models from laser-scanned point clouds: A review of related techniques. *Automation in Construction*, *19*(7), 829–843. https://doi.org/10.1016/j.autcon.2010.06.007

Tatoglu, A., & Pochiraju, K. (2012). Point cloud segmentation with LIDAR reflection intensity behavior. *Proceedings - IEEE International Conference on Robotics and Automation*, 786–790. https://doi.org/10.1109/ICRA.2012.6225224

Te, G., Zheng, A., Hu, W., & Guo, Z. (2018). RGCNN: Regularized graph Cnn for point cloud segmentation. *MM 2018 - Proceedings of the 2018 ACM Multimedia Conference*, 746–754. https://doi.org/10.1145/3240508.3240621

Tsay, G. S., Staub-French, S., & Poirier, É. (2022). BIM for Facilities Management: An Investigation into the Asset Information Delivery Process and the Associated Challenges. *Applied Sciences (Switzerland)*, *12*(19). https://doi.org/10.3390/app12199542

Twin, D. (2022). *Relationship between Digital Twin and Building Information Modeling*.

van Dinter, R., Tekinerdogan, B., & Catal, C. (2022). Predictive maintenance using digital twins: A systematic literature review. *Information and Software Technology*, *151*(February), 107008. https://doi.org/10.1016/j.infsof.2022.107008

Varga, M., & Healthineers, S. (2016). *3D imaging and image processing – literature review*. *May*.

Voas, J. M., Mell, P. M., & Piroumian, V. (2021). *Considerations for Digital Twin Technology and Emerging Standards - Draft NISTIR 8356*. 1–34. https://doi.org/10.6028/NIST.IR.8356-draft

Wang, R., Peethambaran, J., & Chen, D. (2018). LiDAR Point Clouds to 3-D Urban Models : A Review. *IEEE Journal of Selected Topics in Applied Earth Observations and Remote Sensing*, *11*(2), 606–627. https://doi.org/10.1109/JSTARS.2017.2781132

Wicaksana, A., & Rachman, T. (2018). Digital Twin - Towards a meaningful framework. In *Angewandte Chemie International Edition, 6(11), 951–952.* (Vol. 3, Issue 1). https://medium.com/@arifwicaksanaa/pengertian-use-case-a7e576e1b6bf

Xie, Y., Tian, J., & Zhu, X. X. (2020). Linking Points with Labels in 3D: A Review of Point Cloud Semantic Segmentation. *IEEE Geoscience and Remote Sensing*

Magazine, *8*(4), 38–59. https://doi.org/10.1109/MGRS.2019.2937630

Xiong, X., Adan, A., Akinci, B., & Huber, D. (2013). Automatic creation of semantically rich 3D building models from laser scanner data. *Automation in Construction*, *31*, 325–337. https://doi.org/10.1016/j.autcon.2012.10.006

Xu, Y., Hoegner, L., Tuttas, S., & Stilla, U. (2017). VOXEL- and GRAPH-BASED POINT CLOUD SEGMENTATION of 3D SCENES USING PERCEPTUAL GROUPING LAWS. *ISPRS Annals of the Photogrammetry, Remote Sensing and Spatial Information Sciences*, *4*(1W1), 43–50. https://doi.org/10.5194/isprs-annals-IV-1-W1-43-2017

Yang, Y., Fang, H., Fang, Y., & Shi, S. (2020). Three-dimensional point cloud data subtle feature extraction algorithm for laser scanning measurement of large-scale irregular surface in reverse engineering. *Measurement: Journal of the International Measurement Confederation*, *151*, 107220. https://doi.org/10.1016/j.measurement.2019.107220

Zaman, F., Wong, Y. P., & Ng, B. Y. (2017). Density-based denoising of point cloud. *Lecture Notes in Electrical Engineering*, *398*(February), 287–295. https://doi.org/10.1007/978-981-10-1721-6_31

Zhang, J., Cheng, J. C. P., Chen, W., & Chen, K. (2022). Digital Twins for Construction Sites: Concepts, LoD Definition, and Applications. *Journal of Management in Engineering*, *38*(2). https://doi.org/10.1061/(asce)me.1943-5479.0000948

Zhang, J., Lin, X., & Ning, X. (2013). SVM-Based classification of segmented airborne LiDAR point clouds in urban areas. *Remote Sensing*, *5*(8), 3749–3775. https://doi.org/10.3390/rs5083749

Zhang, Z., & Zhu, L. (2023). A Review on Unmanned Aerial Vehicle Remote Sensing: Platforms, Sensors, Data Processing Methods, and Applications. *Drones*, *7*(6), 1–42. https://doi.org/10.3390/drones7060398

Zhao, L., Zhang, H., Wang, Q., & Wang, H. (2021). Digital-Twin-Based Evaluation of Nearly Zero-Energy Building for Existing Buildings Based on Scan-to-BIM. *Advances in Civil Engineering*, *2021*. https://doi.org/10.1155/2021/6638897

Zlatanova, S., Liu, L., Sithole, G., Zhao, J., & Mortari, F. (2014). Space subdivision for indoor applications. In *OTB Research Institute for the Built Environment. Delft,* *Netherlands: Delft University of Technology* (Issue 66).

Zlatanova, S., Yan, J., Wang, Y., Diakité, A., Isikdag, U., Sithole, G., & Barton, J. (2020). Spaces in spatial science and urban applications—state of the art review. *ISPRS International Journal of Geo-Information*, *9*(1), 1–28. https://doi.org/10.3390/ijgi9010058

GeeksforGeeks. (2022, November 28). Convex hull using Jarvis' algorithm or wrapping. GeeksforGeeks. https://www.geeksforgeeks.org/convex-hull-using-jarvis-algorithm-or-wrapping/

.Person, Male, Erzhuo, Che, Michael, & Olsen. (2022, December 21). Lidar Point Cloud Segmentation. GIM International. https://www.gim-international.com/content/article/lidar-point-cloud-segmentation

Appendix A

A .1 Overlapping wall algorithm

```
foreach (var curve1 in mergedLines)
{
     // define first point and last point from each curve in list
     XYZ curveStartPoint = curve1.GetEndPoint(0);
     XYZ curveEndPoint = curve1.GetEndPoint(1);

     XYZ curveLowestXValuePoint;  XYZ curveHighestXValuePoint;

     // sort the intial point along the first and the last point
if (curveStartPoint.X  < curveEndPoint.X)
  curveLowestXValuePoint = curveStartPoint; curveHighestXValuePoint = curveEndPoint;

else
curveLowestXValuePoint = curveEndPoint;   curveHighestXValuePoint = curveStartPoint;

     bool merged = false;  bool isConsidered = false;

     //check the line with already merged lines or not
     foreach (var line in newMergedLines)
     {
             if (line!= curve1 &&
             line.Direction().Normalize().IsAlmostEqualTo(XYZ.BasisX) &&
             Math.Abs(curve1.GetEndPoint(0).Y - line.GetEndPoint(0).Y) <= 0.3)
             {
                isConsidered = true;
             }
     }

// check if the line already checked with the merged lines, so continue
if (isConsidered == false)
{
      // check the line with other lines of all the spaces' boundaries
       foreach (Line otherLine in mergedLines)
       {
      //check if the curves having the same direction and within the same location
      with 0.3 ft

      if (otherLine != curve1
      &&otherLine.Direction().Normalize().IsAlmostEqualTo(XYZ.BasisX) &&
      Math.Abs(curve1.GetEndPoint(0).Y - otherLine.GetEndPoint(0).Y) <= 0.3)
      {
              merged = true;
              List<XYZ> endPoints = new List<XYZ>();

   endPoints.Add(otherLine.GetEndPoint(0)); endPoints.Add(otherLine.GetEndPoint(1));
   endPoints.Add(curve1.GetEndPoint(0));      endPoints.Add(curve1.GetEndPoint(1));
```

```
                XYZ pointWithLowestX = endPoints.OrderBy(p => p.X).First();
                XYZ pointWithHighestX = endPoints.OrderBy(p => p.X).Last();

                //consider the new
                if (curveLowestXValuePoint.X >= pointWithLowestX.X)
                       curveLowestXValuePoint = pointWithLowestX;

                if (curveHighestXValuePoint.X <= pointWithHighestX.X)
                       curveHighestXValuePoint = pointWithHighestX;
                }

            }
       }
              // add the new line to the list
                if (merged == false && isConsidered == false)
                      newMergedLines.Add(curve1 as Line);

                if (merged== true && isConsidered == false)

               Line newCurve1 = Line.CreateBound(curveLowestXValuePoint,
               curveHighestXValuePoint);
                newMergedLines.Add(newCurve1);

}
```

A .2 Reliability check algorithm

```
//check if the BB is reliable according to number of points inside that should
exceed specific precentage like 90 %

double reliablityFactor = 0.9;

double numOfPointsInBB = pointsCounterListinBB.Max();

double roomPCPointsCount = roomPCPoints.Count;

double precentageOfExistingPointsInAssumedBB = numOfPointsInBB / roomPCPointsCount;


if (precentageOfPointsInsideBB >= reliablityFactor)
{
      int indexMaxPointsCounterinBB =
      pointsCounterListinBB.IndexOf(pointsCounterListinBB.Max());

      Solid sol = BBList[indexMaxPointsCounterinBB].ToSolid();

      Helper.CreateCuboidFromSolid(doc, sol);

}

else
{
      XYZ startPoint = new XYZ(roomPCPoints.Min(point => point.X),
      roomPCPoints.Min(point => point.Y), roomPCPoints.Min(point => point.Z));

      var BB = Helper.CreateBoundaryBox(doc, startPoint, roomDimensionX,
      roomDimensionY, roomDimesnionZ);

      Solid sol = BB.ToSolid();

      Helper.CreateCuboidFromSolid(doc, sol);

}
```

A .3 Algorithm for extracting internal walls

```
foreach (var point in pointsInWallBB)
{
          IntersectionResult projectionResult = newMergedLines[i].Project(point);

          if (projectionResult != null && projectionResult.XYZPoint != null)
          {
               // Get the projected point
               XYZ projectedPoint = projectionResult.XYZPoint;

               // Calculate the distance btw. the original point and the projected o
               double distance = point.DistanceTo(projectedPoint);

               averageDistances.Add(distance);
          }
 }

 double average = averageDistances.Average();

 double originalNum = average * 2;

 int nearestMultipleOf5 = (int)Math.Round(originalNum / 50.0) * 50;

 if (nearestMultipleOf5 <= 300)
      nearestMultipleOf5 = 300;

 else if (nearestMultipleOf5 >= 500)
      nearestMultipleOf5 = 500;
```

Appendix B

B .1 Convex hull algorithm

```
public static List<XYZ> ConvexHull(this List<XYZ> points)
{
     if (points == null) throw new ArgumentNullException(nameof(points));
     XYZ startPoint = points.MinBy(p => p.X);
     var convexHullPoints = new List<XYZ>();
     XYZ walkingPoint = startPoint;
     XYZ refVector = XYZ.BasisY.Negate();
     do
     {
         convexHullPoints.Add(walkingPoint);
         XYZ wp = walkingPoint;
         XYZ rv = refVector;
         walkingPoint = points.MinBy(p =>
         {
             double angle = (p - wp).AngleOnPlaneTo(rv, XYZ.BasisZ);
             if (angle < 1e-10) angle = 2 * Math.PI;
             return angle;
         });
         refVector = wp - walkingPoint;
     } while (walkingPoint != startPoint);
     convexHullPoints.Reverse();
     return convexHullPoints;
}
```

Declaration of Originality

With this statement, I declare that I have independently completed this master's Thesis. The thoughts taken directly or indirectly from external sources are correctly marked as such. This thesis was not previously submitted to another academic institution and must be published.

München, 5. November 2023 Ahmed Ibrahim

First Name Last Name

Name: Ahmed Ibrahim

Traunsteiner Str. 5

81549 München

ahmed.ibrahim@tum.com